UNIVERSITÀ DEGLI STUDI DI MILANO

Dipartimento di Scienze della Salute

Scuola di Dottorato in Scienze Biochimiche, Nutrizionali e Metaboliche

Dottorato di Ricerca in Fisiopatologia, Farmacologia, Clinica e Terapia delle Malattie Metaboliche
Ciclo XXVIII

Purification, characterization and culture of ensheathing cells from human olfactory mucosa biopsies

Dottorando: Filippo Caremoli
Matricola: R10251

Coordinatore: Professor Alfredo Gorio

Tutor: Professor Alfredo Gorio

Anno Accademico 2014/2015

“Lascio questa scrittura, non so per chi,

non so più intorno a che cosa:

***stat rosa pristina nomine, nomina nuda tenemus*”**

(da “Il nome della rosa” di U. Eco)

“Tutto questo è molto italiano”

(Stanis La Rochelle)

Dedicato a chi

ha creduto in me

e nelle mie possibilità

INDEX

SUMMARY

Among all the possible sources of mesenchymal stem cells, adipose tissue and olfactory mucosa have raised great interest and have become some of the most investigated sources.

Adipose tissue-derived mesenchymal stem cells and the fat itself as a source of human adipose derived stem cells, represent one of the major fields of research in regenerative medicine. A great advantage is represented by the minimal invasive and high accessibility to adipose tissue and its ready availability. In the present study, hADSCs were isolated from the adipose tissue donated by several patient and have been investigated and characterized through different technical approaches, such as flow cytometry and immunocytochemistry. These hADSCs reproducibly fulfill the general definition of MSCs by both phenotypic and differentiation capabilities criteria, showing also the expression of neural markers, as observed by confocal microscope analysis. Lipoaspirated adipose tissue showed positivity to ß-tubulin III that was also maintained in lipoaspirate-derived hADSCs. A population of stem cells retaining typical characteristics of surface markers of classical adipose tissue stem cells and MSC was obtained when adipose tissue was subjected to culture in vitro, either by processing through centrifugation or by direct plating without enzymatic digestion with collagenase. Flow cytometry analyses showed that hADSCs expressed classical mesenchymal markers such as CD44, CD73, CD90, CD105 and CD166, while endothelial (CD31, CD34, CD144, CD146) and hematopoietic (CD45, CD133) markers were much less represented. Also the ability to give rise to tissue of mesenchymal origins, such as osteoblastic and adipogenic lineages, were present in hADSCs. In addition, the immunofluorescence staining indicated the expression of neural stem markers in hADSCs which consequently co-expressed nestin, β-tubulin III and glial GFAP.

We have also characterized human olfactory Ensheathing stem cells. Olfactory mucosa is specialized tissue inside the nasal cavity involved in olfactory perception and capable of lifelong regeneration throughout adulthood. Multipotent stem cells obtained from it offer the possibility of promoting

regeneration and reconstruction in regenerative medicine, being readily accessible with minimal invasive techniques, capable of expansion *in vitro* and retaining broadly potent differentiative capacity as stem cell progenitors. Among the several members of the olfactory mucosa, Olfactory Ensheathing Cells (OECs) are well known to be useful in repairing the nervous system. By following our method, cells can be easily isolated and maintained in TCM, and their cultivation in large flasks allowed obtaining rich cultures of OECs in 2 weeks. Cell cycle analysis showed that the majority of cells are in G0/G1 phase, while just a lesser part is in S/G2 phase. In our growth conditions, no chromosomal abnormalities were observed also at high culture passage (p14). Live morphology of obtained cells showed a fibroblast-like phenotype and the immunohistochemical analyses showed the expression of beta-Tubulin III, Vimentin, Nestin, Glial Fibrillary Acidic Protein and Microtubule-Associated Protein 2. By FACS analysis we demonstrated that OECs are positive to typical surface mesenchymal markers (CD44, CD73, CD90, CD105, CD146 and CD166). As expected, some endothelial (CD31, CD34) and hematopoietic (CD45) markers were very few represented, while some others (CD56, CD144, CD146, CD133) are partially found. These cells also express genes that constitute the core circuitry of self-renewal such as SOX2, NANOG and OCT4 and the stemness marker CD133. OECs incubated with serum-free medium, normally used for the formation of neurospheres, spontaneously formed large spheroids reaching a mean diameter of 100 μm in 10 days of culture. Immunofluorescence of specific proteins showed that spheres were positive to markers such as Nestin, Vimentin, TUJ-1, MAP2 and GFAP.

In conclusion, our method allows the quickly and easily hADSCs and hOESCs isolation from human adipose tissue and nasal biopsies. The obtained cells can be cultured without altering their mesenchymal properties, suggesting the pluripotency nature of these cells and that they are a reliable source for regenerative medicine.

1 INTRODUCTION

1.1 Regenerative Medicine

Regenerative medicine is a promising and topical field of biomedical research that seeks to combine the knowledge and expertise of diverse disciplines, i.e. cellular and molecular biology, tissue engineering and clinical translational medicine, with the aim of healing the body malfunctions [1]. The regeneration of tissues and organs is a new strong approach to treat various diseases and injuries, in contrary to the regenerative medicine, which aims not only to replace what is malfunctioning, but also to provide the elements required for in vivo repair, seamlessly interacting with the living body and stimulating its intrinsic regenerative capacities [2]. Under this light, regenerative medicine is an emerging interdisciplinary area of research and clinical applications focused on the repair, replacement, or regeneration of cells, tissues, or organs to restore impaired function resulting from any cause, including congenital defects, disease, and trauma. It uses a combination of several technological approaches that moves it beyond traditional transplantation and replacement therapies. These approaches may include, but are not limited to, the use of stem cells, soluble molecules, genetic engineering, tissue engineering, and advanced cell therapy.

The United States National Academies of Science report, Stem Cells and the Future of Regenerative Medicine, estimates that the potential patient populations in the US for stem cell–based therapies include more than a hundred million patients with conditions such as cardiovascular disease, autoimmune diseases, diabetes, cancer, neurodegenerative diseases, and burns [3].

The current approaches are influenced by our understanding of embryonic development, of tissue turnover and replacement in adult animals and by tissue engineering and stem cell biology [4] [5], [6].

Stem cells are a key component of regenerative medicine, as they open the door to new clinical applications. For a successful application of stem cell-based approaches, it is necessary to define the scientific and clinical advances, as well as regulatory, ethical, and societal issues in terms of safety and efficacy [8]. Considering the large number of improved protocols of cells differentiation and the increasing availability of human multipotent stem cells, the prospect of an access to unlimited numbers of specific cell types on demand could become a reality for several diseases. Up-to-date advances in stem cell field are suggesting that the direct use of cells could really be translate into effective therapies for currently unmanageable disorders, although the road towards translation in humans is still full of new challenges [101].

The regeneration of organs and appendages after injury occurs in diverse animal groups and provides another important viewpoint, in addition to the demonstration that complex adult tissues can be rebuilt. Regenerative medicine currently uses three approaches: the implantation of stem cells to build new structures, the implantation of pre-primed cells already committed to a given direction, and the stimulation of endogenous cells to replace missing structures [7]. Endogenous cells must evoke each of the different aspects identified in the first two approaches, the generation of an appropriate cohort of regenerative cells, their regulated division and differentiation, and the restoration of the appropriate part of the structure.

So far, stem cell therapy has only been established as a clinical standard of care for diseases of the blood system. However, there is an increasing number of clinics testing stem cell interventions, some of them offer stem cell treatments for a variety of conditions without clear evidence of safety or efficacy. For the successful application of novel stem cell-based approaches, it will be necessary to define the scientific and clinical advances, as well as the associated regulatory, ethical, and societal issues, that need to be addressed in order to deliver treatments safely, effectively, and fairly [8].

1.2 Embryonic Stem Cells and Adult Stem Cells

ESCs are the target of regeneration research for their unique pluripotency, which can not be seen in any other types of stem cells. They are isolated directly from blastocyst in the early stage of embryonic development by mechanical or laser dissection. Unlike adult stem cells are ESCs able to self renew an unlimited number of times and can give rise to all three germ layers and potentially differentiate into every kind of cells [100].

Two characteristics distinguish stem cells from other cell types: the ability to self-renew and to differentiate into multiple lineages. ESCs are pluripotent cells derived from the inner cell mass of the blastocyst during early embryogenesis [9] [10]. They are unique for the ability to form all cell types in the human body and self-renew indefinitely and thus have been extensively investigated in the area of regenerative medicine since their isolation 30 years ago. However, ethical considerations, technical challenges, and governmental regulations have hindered their use [11]. As a result, the study of somatic or adult stem cells, which does not generate the same ethical concerns, has increased dramatically. Unlike ESCs, adult stem cells are characterized by a restricted differentiation potential and finite self-renewal.

They originate from embryonic stem cells; during gastrulation three germinal layer are formed and the progeny of embryonic stem cells is separated into distinct groups of precursors, which gradually mature into those that will be considered stem cell organ-and tissue-specific (somatic). Somatic stem cells can be isolated from various mammalian tissues throughout the period of fetal development and from adult tissues, even though their number gradually decreases until reaching minimum values in adulthood.

Adult stem cells have been localized in many types of tissue including mesenchymal [12], neural [13], gastrointestinal [14], hepatic [15], gonadal [16] [17], and hematopoietic [18]. Their predominant function is to contribute to the maintenance of tissue homeostasis, generating a progeny of

differentiated cells to replace mature cells lost due to injury or physiological renewal. The extent to which stem cells perform this function can change significantly by tissue type; for example tissues such as epidermis, epithelium of small intestine and hematopoietic system are subject to a continuous cell renewal.

Adult stem cells remain in a non-proliferative, quiescent state during most of their lifetime until stimulated by the signals triggered by tissue damage and remodeling [19] [20]. Upon stimulation, adult stem cells re-enter the cell cycle to replenish the stem cell pool, as well as to generate progenitor cells, which then give rise to a variety of differentiated cell types for tissue regeneration and homeostasis. The number of stem cells within a particular tissue is not regulated at the level of single cell but to the cell population. Stem cells perform symmetrical divisions in which the two daughter cells are identical (division expansive) or, alternatively, different from the mother cell stem (division differentiative). The self-maintenance is guaranteed by numerical balance between the two types of symmetric division with the population.

A second model, called deterministic, provides that a single stem cell given rise, each mitotic division, to two daughter cells of which at least one is identical of the parent cell. This type of division is said asymmetric because the two daughter cells follow different paths of development. This model guarantees the retention of a stable number of stem cells and the production of differentiated cells. Most of the stem cells using both methods and the balance between them are controlled by the stage of development of the organism and by environmental factors [21].

Cytokines, growth factors, adhesion molecules, and extracellular matrix components in the stem cell microenvironment play important roles in stem cell fate determination, working as the driving forces to switch from a self-renewal to a differentiation stage [22] [23] [24] [25] [26]. However, the downstream intracellular effectors in these processes are still largely unknown.

In addition to self-renewal and multipotency, adult stem cells possess the ability to trans-differentiate, defined as the capability to switch from their specific developmental lineage into another cell type of a different lineage, sometimes across embryonic germ layers. For example, mesenchymal stem cells (MSCs) can be induced to become non-mesodermal cells, including functional neurons, astrocytes, oligodendrocytes, and endothelial cells, by appropriate extrinsic stimuli both in vitro [27] [28] [29] [30] and in vivo [31].

The first isolated and studied adult stem cells were hematopoietic stem cells resident in the bone marrow, but in the ‘70s another cell population was found in rats and guinea pig bone marrows and they were called stromal fibroblasts of mesenchymal origin, hereafter said mesenchymal stem cells (MSCs) [32].

1.3 Mesenchymal stem cells

Mesenchymal stem cells (MSCs) are a great therapeutic cell source. MSCs are adult stem cells that belong to the mesodermal lineage and are traditionally found in the bone marrow as bone marrow mesenchymal stem cells (BMSCs). MSCs can also be isolated from other mesenchymal tissues, such as umbilical cord, dermis, adipose tissue, and peripheral blood. They are characterized by long thin cell bodies with a large nucleus similar to that of fibroblasts and they have a high capacity for self-renewal while maintaining multipotency. MSCs can be obtained from patients (for auto-transplantation) as well as from healthy donors (for allo-transplantation).

The story started with Friedenstein and coworkers, in a series of studies in the 1960s and 1970s (and reviewed in [33]), who demonstrated that the osteogenic potential, as revealed by heterotopic transplantation of Bone Marrow cells, was associated with a little subpopulation of these cells. They found a rare cell population in the bone marrow (0,001% - 0,01% of the total) with fibroblast-like morphology and they were able to adhere to the plastic surface of culture plates. Those colonies were

called CFU-F (colony forming unit- fibroblast) and the constituting cells are able to grow without any particular nutritional exigency, except for the presence of fetal bovine serum ([34] [35]. Ten years later they were isolated from human bone marrow [36]. The name 'Bone Marrow Stromal Fibroblasts' has been replaced by 'Mesenchymal Stem Cells' (MSCs) for the first time by Arnold Caplan [37].

MSCs population isolated from the bone marrow are still considered as the gold standard for MSC applications. Nevertheless the bone marrow has several limitations as source of MSCs, including MSC low frequency in this compartment, the painful isolation procedure and the decline in MSC characteristics with donor's age. Thus, there is accumulating interest in identifying alternative sources for MSCs. To this end, for instance, MSCs obtained from the Wharton's Jelly (WJ) of umbilical cords have gained much attention over the last years since they can be easily isolated, without any ethical concerns, from a tissue, which is discarded after birth. Furthermore WJ-derived MSCs represent a more primitive population than their adult counterparts, opening new perspectives for cell-based therapies [38].

In the umbilical cord, hematopoietic and mesenchymal stem cells co-exist. It begins to form in the first month of fetal life, when the cells of morula (development stage when the zygote consists of 8 to 16 cells) that will give rise to the embryo differ from those that will form placenta and the fetal adnexa (amniotic sac and the umbilical cord). Inside the umbilical cord there are three blood vessels: two arteries and one vein. The portal vein brings to the baby oxygen and nutrients, which come from the placenta, while arteries allow the child to eliminate catabolites into the placenta. These three channels are covered with a gelatinous material called Wharton's jelly, seat of the MSCs.

It is now know that MSCs are virtually ubiquitous, representing a component of the stroma of many tissues, such as bone marrow, skin, digestive epithelium, dental pulp, hair follicles, brain, amniotic fluid, placenta, etc. [39] [40]. MSCs are more recently defined by The International Society of Cellular Therapy based on three cellular properties: (1) adherence to plastic, (2) positive expression of CD105,

CD73, and CD90 and negative expression of CD45, CD34, CD14 or CD11b, CD79α or CD19, and HLA class II, and (3) differentiation potential to mesenchymal lineages including osteocytes, adipocytes, and chondrocyte [41].

In addition, human mesenchymal stem cells (hMSCs) are able to maintain their multi-differentiation potential after commitment (**Figure 1**). As demonstrated by Song L. et al. (2004) osteoblasts, chondrocytes, and adipocytes differentiated from hMSCs can trans-differentiate into other cell types in response to extrinsic factors, likely through genetic reprogramming. However, the molecular mechanisms behind the trans-differentiation process are poorly understood.

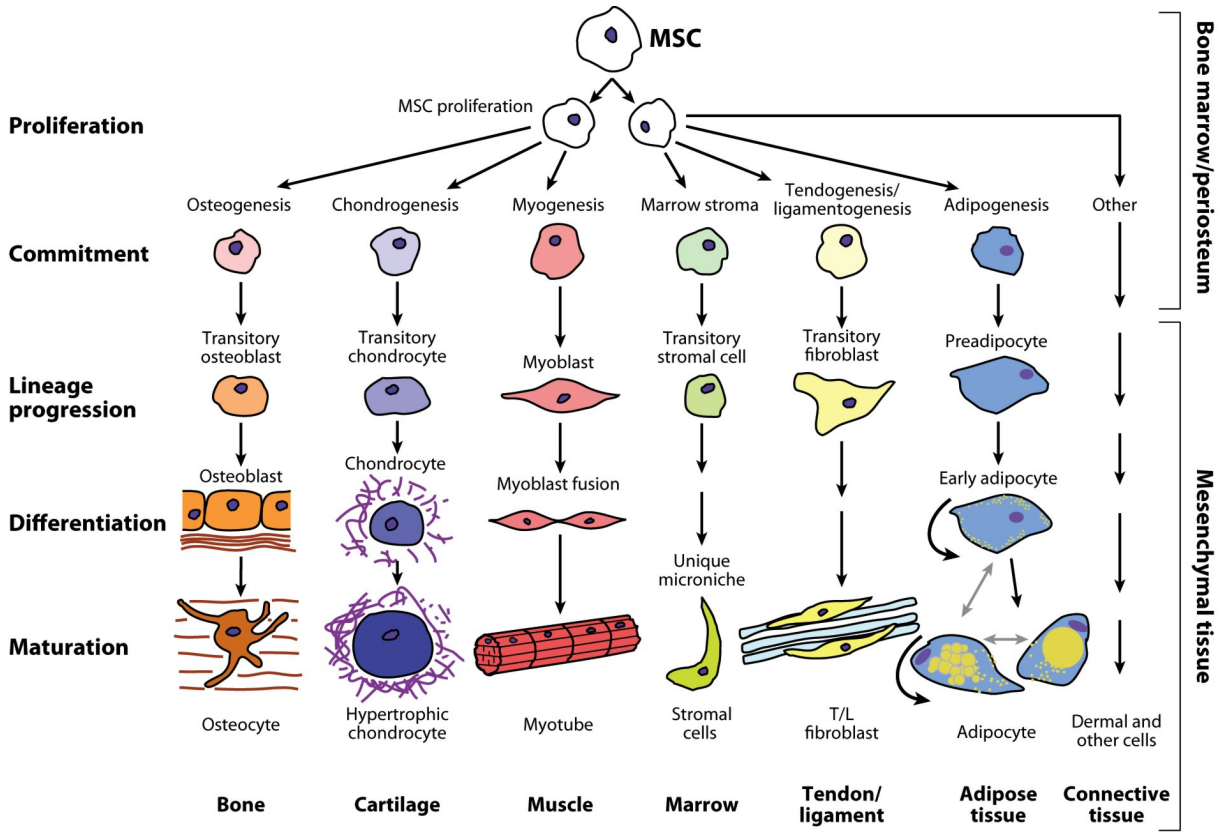

Singer NG, Caplan AI. 2011.
Annu. Rev. Pathol. Mech. Dis. 6:457–78

***Figure 1**: **Mesenchymal stem cells multilineage differentiation potential: the mesengenic process**. Human mesenchymal stem cells (hMSCs) from bone marrow may develop into bone, muscle, or adipose tissue, depending on the stimuli to which they are exposed in vitro. Shown is a hypothesis of the mesengenic process that hMSCs undergo both in vitro and in vivo. From [42].*

The umbilical cord and adipose tissue are other realistic sources of MSCs. Mesenchymal tissue of the umbilical cord, so-called Wharton's jelly, as well as fat tissue, contain an abundance of MSCs. Adipose tissue, which is easily obtained from liposuction, also contains large amounts of MSCs called adipose-derived stem cells (ADSCs).

1.4 Human Adipose Derived Stem Cells (hADSCs)

Recent studies have shown that subcutaneous adipose tissue provides a clear advantage over other MSCs sources due to the ease with which adipose tissue can be accessed (under local anesthesia and with minimum patient discomfort) as well as to the ease of isolating stem cells from the harvested tissue [43].

Stem cells frequency is significantly higher in adipose tissue than in bone marrow [44]. Routinely, $1x10^7$ adipose stromal/stem cells have been isolated from 300 ml of lipoaspirate, with greater than 95% purity [45]. In other words, the average frequency of Adipose Derived Stem Cells (ADSC) in processed lipoaspirate is 2% of nucleated cells, and the yield of ADSCs is approximately 5,000 fibroblast colony-forming units (CFU-F) per gram of adipose tissue, compared with estimates of approximately 100–1,000 CFU-F per milliliter of bone marrow [46].

Subcutaneous adipose tissue samples can generally be obtained under local anesthesia. Current methods used for isolating ADSCs rely on collagenase digestion followed by centrifugal separation to isolate the SVFs from primary adipocytes. They display a fibroblast-like morphology and lack the intercellular lipid droplets seen in adipocytes. Isolated ADSCs are typically expanded in monolayer culture on standard tissue culture plastics with a basal medium containing 10% fetal bovine serum [47]. The proliferation capacity of ADSCs seems to be greater than that of bone marrow-derived MSCs.

Previous reports have shown that the doubling times of ADSCs during the logarithmic phase of growth range from 40 to 120 hours [48] [49] [50] are influenced by donor age, type (white or brown adipose

tissue) and location (subcutaneous or visceral) of the adipose tissue, the harvesting procedure, culture conditions, plating density and media formulations [51]. Based on beta-galactosidase activity, senescence in ADSCs is similar to that in bone marrow-derived MSCs [49]. ADSCs possess the potential to differentiate toward a variety of cell lineages both in vitro and in vivo [52], and some of the research has been passed on to patients in the form of clinical trials [53]. Although ADSCs are of mesodermal origin, it is now clear that they can differentiate into ectoderm and endoderm lineage cells as well as mesoderm (revised in [54]). It has been shown that hADSCs are able to differentiate into the classical mesodermal tissues like bone, fat and cartilage [48] [55]), and it is claimed that they can be differentiate into nerve, cardiomyocytes, hepatocytes and pancreatic cells [56].

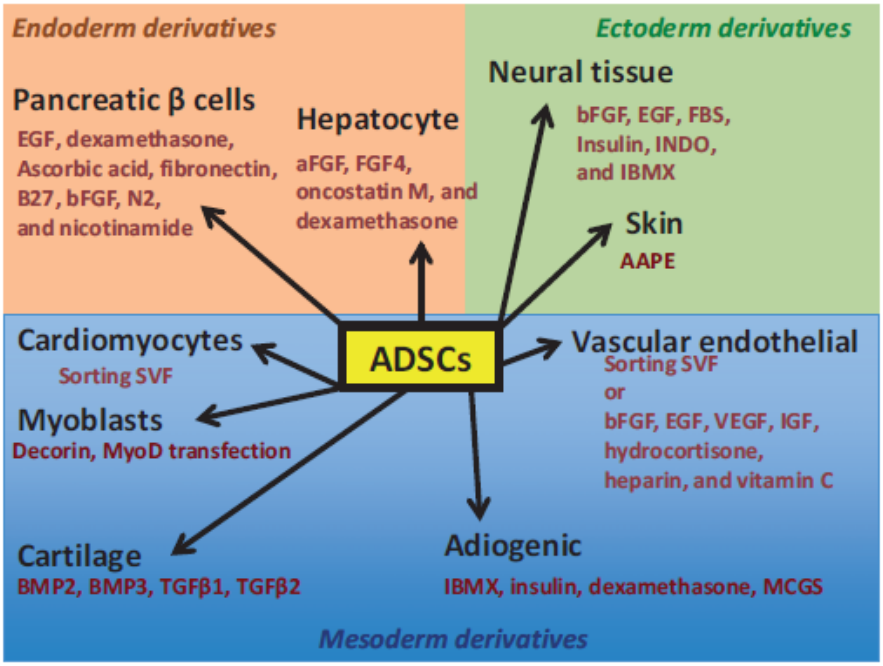

Figure 2: hADSCs differentiation potential.

HADSCs show the same surface markers as bone marrow derived MSCs. The potential of in vivo application of these cells is still unclear, however it has been shown their action on supporting neuronal repair, osteogenesis and vasculogenesis.

In some studies it was demonstrated that hADSCs could release multiple angiogenic growth factors and cytokines/chemokines such as UTF-1, Nodal, and Snail2, which are known to be expressed by embryonic stem cells but have been never described in other stem lineages.

Even though autologous transplant of adipose tissue is an old therapeutic procedure still used to repair a wide range of tissue damages, the recent biological studies performed on stem cells suggest the possibility to significantly improve the potentiality of tissue regeneration by making use of ADSCs.

They represent therefore a promising source for cell therapy, especially as their isolation is less invasive compared to bone marrow extractions, as they can be obtained from lipoaspirate with a noninvasive procedure in abundant quantities and their expansion in culture is quite easy. Moreover they can be transplanted to autologous host. To purify adipose stem cells usually fat was harvested during microliposuction under tumescent local anesthesia using Coleman's microcannulas. Lipoaspirate fat was centrifuged in closed sterile system at 2000 rpm for 10 minutes and the pellet was digested with Collagenase for half an hour at 37°C (**Figure 2**). The digest was centrifuged, separating the floating population of mature adipocytes from the pelleted stromal vascular fraction (SVF). After 24-hour plating in standard medium (Dulbecco's Modified Eagle Medium supplemented with 10% fetal bovine serum, penicillin (100 U/mL), and streptomycin sulfate (100 μg/mL), non-adherent cells are removed. The plastic-adherent cell population identifies the adipose tissue–derived stromal cells (ADSCs).

1.5 Human Olfactory Ensheathing Stem Cells (hOESCs)

Olfactory mucosa/epithelium is a specialized tissue inside the nasal cavity that is involved in olfactory perception. It is a tissue capable of lifelong regeneration throughout adulthood and Multipotent stem cells obtained from it offer the possibility of promoting regeneration and reconstruction in regenerative

medicine, being readily accessible with minimal invasive techniques [57] [58] and retaining broadly potent differentiative capacity as stem cell progenitors [59].

Among the several components of the olfactory mucosa, two types of cells are known to be useful in repairing the nervous system, i.e. stem-like progeniors cells and Olfactory Ensheathing cells (OECs). Within the nasal cavity, OECs are found in the mucosa of superior turbinate, nasal septum and middle turbinate [75].

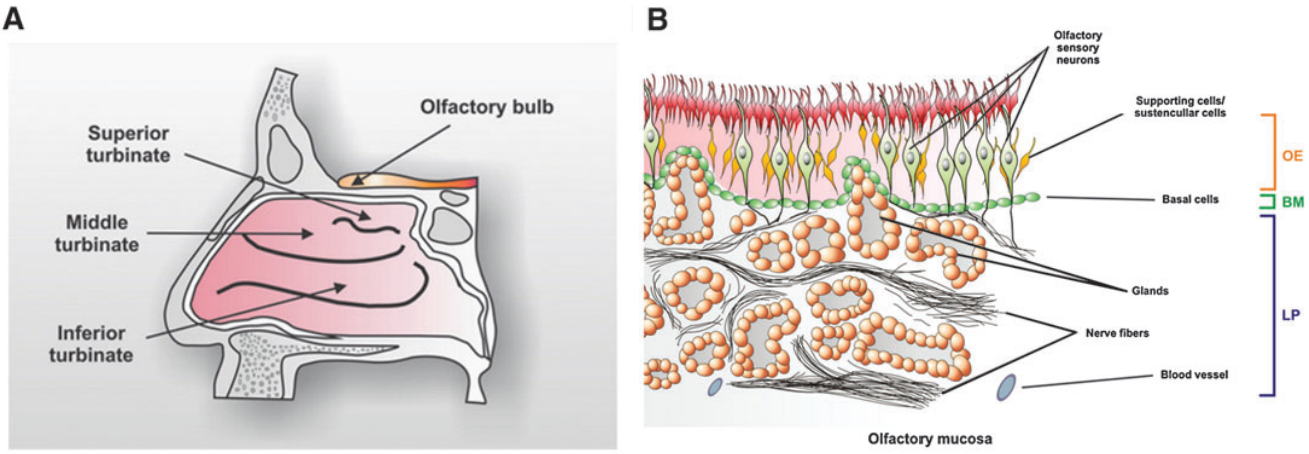

Figure 3: Olfactory mucosa*. (A) Turbinates localization (B) Schematic illustration of the morphology of Olfactory epithelium. OE: Olfactory epithelium. BM: basement membrane. LP: Lamina propria. (taken from [79])*

OECs are specific class of glial cells, which are restricted to both the PNS and CNS, and share certain characteristics with astrocytes as well as Schwann cells [60]. OECs are present in the olfactory epithelium, where neurogenesis occurs throughout adulthood. The olfactory epithelium (OE) is composed of two kinds of neural stem cells, which are the globose basal cells (GBCs) and the horizontal basal cells (HBCs). GBCs are the main resource for homeostatic neurogenesis that leads to the birth of neurons and other cellular populations such as OECs. Unlike the GBCs, HBCs are normally quiescent, but they can be activated to generate novel GBCs to reconstruct the cellular populations of OE after injury. [61] [62]

OECs were identified by their elongated shape with thin laminar processes that ensheath olfactory nerves in situ, but the morphologies of cultured OECs are distinct, from flat shape to bipolar and tripolar, moreover, there are also various antigenic differences. These heterogeneities may be caused by the different origins of the olfactory tissue used, the age of donor, the method of isolation, and culture conditions, and can also be affected by extracellular and intracellular molecules. This kind of property is thought to allow OECs to transform themselves within different morphological and antigenic types to exhibit different functions and to adapt various environments. [63] [76] [77] [78]

Nevertheless, compared with Schwann cells, OECs are more likely to rescue neural function in the injured spinal cord by virtue of their cell-specific properties. The bridging effect of transplanted OECs on regenerated axons of dissected dorsal root into spinal cord was reported by Li et al. [64]

In a previous study, Murrell *et al.* showed that human olfactory lamina propria derived stem cells can be (1) grown in large numbers and (2) differentiated into neural and non-neural cell types in vitro and in vivo. These cells can give rise to mesodermal cell types, a feature never reported with neural stem cells and therefore, as resident of a connective tissue originating from a mesenchyme, this cell type could be part of the family of MSCs. [80]

The open list of tissues that produce MSCs can be updated with the inclusion of the olfactory lamina propria-derived stem cells, termed as olfactory ectomesenchymal stem cells. The olfactory lamina propria is a relatively thick layer of connective tissue that originates from the fronto-nasal mesenchyme [81][82], itself arising from the interaction of cranial neural crest and olfactory placodes [83].

It is therefore not a surprise to identify, within this tissue, MSCs with ectodermal characteristics. This finding is in line with previous reports describing neural crest-derived MSCs, found in the branchial arch during development and in the teeth during adulthood, and named ectomesenchymal stem cells [84]. Interestingly, it has been shown that olfactory ectomesenchymal stem cells (also named "mesenchymal–neural" precursors) have the capacity to differentiate into ectoderm and mesoderm cell

types [85].

In a study, Hauser et al. show that the human respiratory mucosa of the Inferior Turbinate contains a novel neural crest-derived stem cell population. Such isolated stem cells from the human respiratory mucosa were able to proliferate and generate primary and secondary neurospheres in suitable cultivation media and both neurospheres contained cells that differentiate into cells of neuro-ectodermal and mesodermal phenotype and could be efficiently directed into neuron-like cells. [79]

Within the nasal cavity, one of the better studied adult stem cell type are the Olfactory Ensheathing Cells (hOESCs) [86] [87]. Genetic assays demonstrated that OECs are formed directly from neural crest cells and, therefore, are neural crest-derived [89]. These so-called olfactory mucosa mesenchymal stem cells expressed high levels of nestin, CD54, and CD90 [90]. In addition, these particular cells could successfully be differentiated towards osteogenic and adipogenic direction, while no chondrogenic differentiation was observed.

1.6 hOESCs transplantation capabilities in SCI (and other CNS diseases)

Most of the efforts of regenerative and translational medicine are addressed to biomedical approaches and clinical therapies that may involve the use of stem cells and cell therapies. One of the best studied applications of cell transplantation is with Spinal Cord Injury (SCI).

SCI is caused by direct mechanical damage to or resection of the spinal cord that results usually in complete or incomplete loss of neural functions, such as mobility and sensory perception [94] [95]. The peculiar properties and the plasticity of hOESCs may allow them to transform themselves within different morphological and antigenic types, resulting in different functions and adaptation features to different environments and animal models [96] [97] [98].

As a result of years of research on animal models of SCI, finally hOESCs came to human clinical trials applications. In 2006 the first pilot clinical study with transplantation of autologous hOESCs [99] were

settled, where seven patients ranging from 18 to 32 years of age were treated at 6 months to 6.5 years after injury and improved their sensory neurological scores. Following this, three studies focused the attention of the scientific community for the transplantation of hOESCs in SCI: in 2013 two studies assessed the safety and feasibility in patients with complete and incomplete thoracic [102] and cervical [103] SCI, giving as a result that, in one year of observation, all treated patients had statistically significant neurological improvements. In 2014, the same group that treated thoracic SCI published a clinical study where a 38-year-old man with a traumatic transection of the thoracic spinal cord was transplanted with an autologous culture containing olfactory Ensheathing cells and olfactory nerve fibroblasts [104]. In this trial, no adverse effects were found at 19 months post-transplantation and the patient improved his neurological scores, with an improved trunk stability, the partial recovery of the voluntary movements of the lower extremities, and an increase of the muscle mass in the left thigh, as well as partial recovery of superficial and deep sensation. This pattern of recovery suggested functional regeneration of both efferent and afferent long-distance nerve fibers, also confirmed by imaging and neurophysiological examinations. Notably, hOESCs can be used not only to treat SCI, but also other CNS diseases like Parkinson's Disease [105] [106] and hippocampal lesions [107].

In summary, OECs exercise their favorable influence on the treatment of CNS injury by several potential mechanisms. Their beneficial influence can be summarized as follows: (1) transplants of OECs might create a permissive microenvironment suitable for axonal regeneration and help to preserve the function and viability of nerve fibers in adjacent tissue; (2) OECs may produce a large amount of neurotrophic substances to promote neuron regeneration; (3) OECs reduce production of inhibitory factors from microenvironment by their morphological plasticity, phagocytosis, migration or can remyelinate spared axons with damaged myelin sheaths. Thus, OECs represent arguably one of the leading candidates for transplant-mediated repair of CNS injury, even if the mechanism(s) by which they exert their beneficial effects remain to be clarified.

2 AIMS OF THE STUDY

The aim of this thesis is to characterize two types of stem cells (hADSCs and hOESCs) in terms of pluripotency features and to foresee their potential role as a cell therapy approach in regenerative medicine.

Detailed aims of the study:

- **Isolation and characterization of hADSCs**

  Human Adipose Derived Stem Cells will be isolated from human lipoaspirated adipose tissue. Lipoaspirate will be investigate for its immunohistochemical features and the derived cells will be characterized for their growth capabilities, expression of superficial markers, pluripotency and *in vitro* differentiation potential.

- **Isolation and characterization of hOESCs**

  Human Olfactory Ensheathing Stem Cells will be isolated from human olfactory mucosa. The derived cells will be characterized for their growth capabilities, expression of superficial markers, pluripotency and sphere formation capability.

3 MATERIALS AND METHODS

3.0 Ethical disclosure

Institutional Review Board, according to local and international guidelines, approved the study.

3.1 HUMAN SUPERIOR TURBINATE TISSUE

3.1.1 Human Superior turbinate tissue collection and isolation

Specimens were obtained from 9 volunteers (8 males and 1 female) who were planned to undergo septoplasty, rhinoplasty and/or functional endoscopic sinus surgery. All patients signed an informed written consent and were enrolled at the Otolaryngology Unit of the San Paolo Hospital, University of Milan, Milan, Italy. Mean age was 37.33 ± 11.24 years (18 min - 56 max). All patients were negative for HIV (Human Immunodeficiency Virus 1 and 2), HCV (Hepatitis C Virus), HBV (Hepatitis B Virus). Patients with neoplasm or nasal polyps were excluded

Each specimen (3-4 mm^2), one per patient, was collected under general anesthesia during nasal surgery. Using a 0° endoscope, the mucosa and *lamina propria* from the posterosuperior septum or the superior nasal concha was incised vertically with a number 11 blade, dissected with a Freer elevator and collected with a Hartmann forceps.

The medium used for Specimens and primary cultures was TCM Medium, consisting in Dulbecco's Modified Eagle's Medium (Gibco®Life Technologies, Italy), Ham F-12 (Gibco®Life Technologies, Italy) supplemented with 10% Fetal Bovine Serum (FBS, Gibco®Life Technologies, Italy) and 1% Penicillin/Streptomycin solution (Gibco®Life Technologies).

Procedure for isolation and expansion of Olfactory epithelium Stem cells were conducted in a Biological Safety Cabinet (BlueBeam4, Belstar, Tradate, VA, Italy) and culture procedures were

carried out at 37°C, 5% CO_2 in a humidified incubator (Certomat® CS-18 Sartorius Stedim, Analytical Service, Cassina de' Pecchi, MI, Italy).

Biopsy tissues were immediately placed on ice in TCM, and then transferred in Dispase II Solution (PluriSTEM™ Dispase-II Solution, Merk-Millipore) 1 mg/mL. After 1 hour at 37°C, olfactory mucosa and *lamina propria* were dissociated brushing gently with a lancet. The remaining tissue and lamina were transferred into a Collagenase I solution (Sigma-Aldrich) 0.25 mg/mL and left 10 minutes at 37°C. Meanwhile, the Epithelium/Dispase solution was resuspended 1:10 with PBS 1X (Euroclone) and centrifuged at 520×g for 5 minutes, then the supernatant was discharged and the pellet resuspended in TCM. The Lamina/Collagenase solution was resuspended 1:10 with PBS 1X and centrifuged at 520×g for 5 minutes, then the supernatant was discharged and the pellet resuspended in TCM. Both resuspended pellets were then placed in the same T-75 Flask (Corning) with appropriate quantity of TCM medium.

3.2 HUMAN OLFACTORY EPITHELIUM STEM CELLS

3.2.1 hOESCs culture and maintenance

After approximately 1 weeks of culture, cells started to migrate from the biopsy and after 2-3 weeks circa they reached confluence. When 80-90% confluence was reached, cells were harvested by 0.05% trypsin/EDTA solution (Euroclone or Gibco® Life Technologies), collected by centrifugation (520×g for 5 minutes) and re-seeded in subconfluent condition. When continuously cultured, medium was changed every 3-4 days.

Freezing was performed resuspending cell pellet in FBS with 10% dimethyl sulfoxide (DMSO, Sigma-Aldrich) and freezing at -80°C, while de-freezing was performed by quickly thawing at 37°C and assessing viability by Trypan Blue dye (Sigma-Aldrich) exclusion assay.

3.2.2 G-banding karyotype analysis

Cytogenetic analyses were performed on "in situ" cultures, obtained by inoculating hOESCs directly onto a coverslip inside Petri dishes (Corning) containing 2 ml of αMEM. Cells were treated with 0.02 μl/ml of Colcemid (Life Technologies Carlsbad, California, USA) for 90 minutes, then treated with hypotonic solution (1:1 Na citrate 1%: NaCl 0.3%) (Sigma-Aldrich St. Louis, MO, USA) and fixative solution of 3:1 methanol:acetic acid (VWR International Radnor, Pennsylvania, USA), replaced twice. At least twenty-five QFQ banding metaphases were observed for each sample. The images were acquired using a fluorescence microscope (BX 60 Olympus) and analyzed with Powergene PSI system.

3.2.3 Cell Growth Analysis

Analysis of growth curve was performed counting the proliferative capacity of Olfactory epithelium Stem cells (hOESCs) obtained from human Superior turbinate tissue from 3 patients maintained in culture in TCM. The analyses were performed starting from cells at culture passage 1. Cells were seeded onto 48-well culture plates (Corning) and maintained in culture in growth medium. At 85% confluence, live cells were counted by Trypan blue (Sigma-Aldrich St. Louis, MO, USA) exclusion test. Cell doubling times (DT) and cell doubling number (CD) were calculated from haemocytometer counts (Neubauer Chamber, VWR International Radnor, Pennsylvania, USA) and cell culture time (CT) for each passage by the following formula: $CD = \ln(Nf/Ni)/\ln 2$ and $DT = CT/CD$, where Nf the final number of cells, and Ni the initial number of cells. The analysis was performed at least three times for each point reported in the curve.

3.2.4 RNA Extraction and qRT-PCR analyses

Total cellular RNAs were extracted using TRI Reagent® (Sigma-Aldrich, St. Louis, MO, USA), according to the manufacturer's instruction. RNA purity and quantity were assessed by Nanodrop (Fisher Scientific) (A_{260}/A_{280} 1.8-2 was considered suitable for further analysis), possible contaminating DNA was removed, and cDNA was prepared from 2.5 µg of RNA using iScript™ Reverse Transcription Supermix for RT-qPCR (Bio-Rad Laboratories, Hercules, CA, USA) according to manufacturer's instruction.

Quantifications of all gene transcripts were performed by real-time retro-transcriptional polymerase chain reaction (Real Time RT-PCR) using iTaq™ Universal SYBR® Green Supermix (Bio-Rad Laboratories) according to manufacturer's instruction and MicroAmp® Fast Optical 48-Well Reaction Plate (Applied biosystems® - Life Technologies Carlsbad, California, USA) on Step One Real-Time PCR System 48 wells (Applied Biosystems) for the expression of 18S rRNA as the internal control. The primer pairs used were: a) SOX2, NM_003106.3; b) NANOG, NM_024865.3; c) OCT4, NM_002701.4; d) CD133, NM_006017.2 (Life Technologies Carlsbad, California, USA). Primer sequences are reported in **Table 1**.

PCR conditions consisted of 1 cycle of 50 °C for 2 minutes, followed by exposure at 95 °C for 10 minutes, 40 cycles of 95 °C for 15 seconds, and 60 °C for 1 minute. 18S rRNA was used as invariant housekeeping gene. The quantitative expression of genes of interest relative to the housekeeping gene was calculated. This reference gene, which is also known as endogenous control, provided a basis for normalizing sample-to-sample differences. Data were only used if the calculated PCR efficiency ranged between 1.85 and 2.0. Template and reverse transcription negative controls (cDNA from a differentiated cell type - human oral mucosa) were also included in all amplification experiments. As positive controls, we used iPS from fibroblasts reprogrammed to express the four Yamanaka factors (Sox2, Oct4, cMyc, Klf4) [93]

18S F	TTTCGGAACTGAGGCCATGATTAAG
18S R	AGTTTCAGCTTTGCAACCATACTCC
SOX2 F	AATCATCGGCGGCGGCAGGATCGGCCAGAG
SOX2 R	GCCGGCCGCCGCCGCGGTGGAGTTGCCGCC
OCT4 F	CCGGAGGAGTCCCAGGACATCAAAGCTCTG
OCT4 R	CCCCAGGGTGAGCCCCACATCGGCCTGTGT
NANOG F	TTCATTATAAATCTAGAGACTCCAGGATTT
NANOG R	AAATCCTGGAGTCTCTAGATTTATAATGAA
CD133 F	ATGGCCCTCGTACTCGGCTCCCTGTTGCTG
CD133 R	ATGCACTAGTTCAAAGAGAATGCCAATGGG

***Table 1**: Primer sequences used*

3.2.5 Cell Cycle analyses

Cell cycle analyses were performed using propidium iodide (PI) (Sigma-Aldrich St. Louis, MO, USA) incorporation method [65]. Briefly, 5×10^5 cells were collected, fixed for 15 min at 4°C in ice cold (-20°C) 70% ethanol. Fixed cells were resuspended and centrifuged. The cell pellet was treated with RNase (Sigma-Aldrich St. Louis, MO, USA) to remove RNA and stained with 25 µg/ml PI at 37°C for 1 hour in the dark. DNA content was analyzed by Cytomics FC 500 (Beckman Coulter). Under these conditions, quiescent cells (G0/G1) were characterized by the minimal RNA content and uniform DNA content.

3.2.6 Indirect immunofluorescence of hOESCs

Cells seeded onto glass slides (3.5×10^3 cells/cm^2) and grown until 85% confluence were fixed with 4% paraformaldehyde. After saturation (4% BSA, 0.3% Triton X-100) (BSA Sigma-Aldrich St. Louis,

MO, USA, Triton X-100 VWR International Radnor, Pennsylvania, USA) and permeabilization, cells were incubated overnight at 4°C with primary antibodies against human Nestin (Clone #196908, R&D Systems), β-tubulin III (Clone TUJ1, Covance), Microtubule-Associated Protein 2 (MAP2, Chemicon), Vimentin (Polyclonal, Santa Cruz) and GFAP (Polyclonal, Covance). Cells were rinsed and then probed 45 minutes with secondary antibodies Alexa Fluor 488 or 543 anti-mouse, rabbit or goat (Invitrogen, Life Technologies Italia, Monza, Italy). Nuclei were counterstained with DAPI (2 μg/ml in PBS) (Sigma-Aldrich), and glasses were mounted with FluorSave^{TM} (Millipore, Billerica, MA, USA). Images were taken using Leica SP2 confocal microscope with He/Kr and Ar lasers (Heidelberg, Germany). In negative control experiments, primary antibodies were replaced with equivalent concentrations of unrelated IgG of the same subclass. The quantification of positive cells was performed by considering on a minimum of 9 independent fields (3 fields/3 coverslips/treatment) of photomicrographs captured with 20X objective. Total counts of each markers immune-reactive cells were performed and the number of positive cells was expressed as the percentage to the total cells. DAPI supplied the total number of cells being a nuclear staining.

3.2.7 Flow cytometric immunophenotypic analysis (FACS)

Cultures of hOESCs at low and high passages were phenotypically characterized by Fluorescence-Activated Cell Sorting (FACS). Following trypsinization and PBS 1x wash, $1x10^5$ cells were re-suspended in 250 μl PBS w/o Ca^{2+} and Mg^{+} for 30 minutes at 4°C in the dark for staining with the following antibodies: anti-CD44 (BD Biosciences Italy), anti-CD90 (Millipore Italy), anti-CD34 (Mylteni Biotec Italy), anti-CD45 (BD Biosciences Italy), anti-CD146 (Biocytex USA), anti-CD31 (Mylteni Biotec Italy), anti-CD56 (Mylteni Biotec Italy), anti-CD105 (Serotec USA), anti-CD144 (R&D System USA), anti-CD166 (BD Biosciences Italy), anti-CD133/2 (Mylteni Biotec Italy), anti-CD73 (BD Biosciences Italy), anti-VEGFR2 (R&D System USA). Samples were fixed with

paraformaldehyde 4% (Sigma-Aldrich St. Louis, MO, USA) and then analyzed by flow cytometry (FACS Vantage, BDBioscience) using CellQuest Pro software (BD Bioscience). For negative controls primary antibodies were omitted. After centrifugation with 1 ml of PBS 1X at 1300×g for 10 minutes, cells were fixed with 4% paraformaldehyde (Sigma-Aldrich, St. Louis, MO, USA) and about 5×10^3 events were acquired for each sample. Non-viable cells were excluded by physical gating. The results of the analysis were expressed as mean ± SD.

3.2.8 Spheroid Formation

hOESCs obtained were grown in TCM medium as described to reach 85% confluence at low passages (<5). After trypsinization, cells were seeded in a 6-well plate ($5x10^3$/well) in neurosphere-medium containing bFGF (20 ng/ml) and EGF (10 ng/ml) in absence of serum [66]. For passaging, spheroids were mechanically dissociated by gentle pipetting and transferred in a new well at the same cell dilution described above. For the immunofluorescence assays, spheres were fixed with formaldehyde 4% and permeabilized with 0.1% Triton X-100, then incubated overnight at 4°C with the following primary antibodies: human Nestin (Clone #196908, R&D Systems), β-tubulin III (Clone TUJ1, Covance), Microtubule-Associated Protein 2 (MAP2, Chemicon), Vimentin (Polyclonal, Santa Cruz) and GFAP (Polyclonal, Covance). The spheres in suspension were rinsed, and subsequently probed 45 minutes with secondary antibodies Alexa Fluor 488 or 543. Nuclei were counterstained with DAPI (2 μg/ml in PBS). Stained spheres were spotted on glasses and mounted with FluorSave™. Images were taken using Leica SP2 confocal microscope with He/Kr and Ar lasers. In negative control experiments, primary antibodies were replaced with equivalent concentrations of unrelated IgG of the same subclass.

3.2.9 Statistical Analysis

Data are expressed as means ± SEM. Two-way analysis of variance (ANOVA) and Bonferroni's post-test were applied using Prism 5 software (GraphPad Software Inc, La Jolla, USA) assuming a p-value less than 0.05 as the limit of significance.

3.3 ADIPOSE TISSUE

3.3.1 Human Adipose tissue collection and isolation

Thirty subjects (11 males and 19 females, between 28 to 80 years) were enrolled at Istituto Image (Milan, Italy). An informed consent was obtained from all the patients**.** All specimens were verified for the presence of HIV (Human Immunodeficiency Virus 1 and 2), HCV (Hepatitis C Virus), HBV (Hepatitis B Virus) and cytomegalovirus. All specimens resulted negative.

Human adipose tissue samples were obtained from elective liposuction procedures under local anesthesia (Lidocaine, AstraZeneca London, United Kingdom). This procedure involved an infiltration step, in which a solution of saline and the vasoconstrictor epinephrine (2 µg/ml) (Key Customer Solutions S.A.S, Basiglio, Milan, Italy) were infused into the adipose compartment to minimize blood loss and contamination of the tissue by peripheral blood cells. The final product was termed lipoaspirate adipose tissue (Lipoaspirate). Lipoaspirate could be directly seeded on a plate or pellet was seeded after centrifugation (920 x *g* for 10') to obtain cells.

The following media were used:

- αMEM (Euroclone, Pero, MI, Italy) supplemented with 20% FBS, antibiotics (1% Penicillin/Streptomycin, 0.3 % Amphotericin B) (Euroclone, Pero, MI, Italy) and L-Glutamine (1%) (Euroclone, Pero, MI, Italy).

- Stem Cells Medium (SCM): DMEM/F12 (Euroclone, Pero, MI, Italy), 20 μg/L human recombinant epidermal growth factor (EGF, Life Technologies Carlsbad, California, USA) and 10 μg/L basic fibroblast growth factor (bFGF; Life Technologies Carlsbad, California, USA), 2 mmol/L L-glutamine, 33 mmol/L glucose, 9.26 g/mL putrescine, 6.3 μg/L progesterone, 5.3 μg/L sodium selenite, 0.0025 g/L insulin, and 0.1 g/L grade II transferring sodium salt (Sigma, St Louis, MO, USA) [114] supplemented with 10% FBS and antibiotics (as above).

Lipoaspirate could be also cryopreserved.

3.3.2 Culture of cryopreserved Lipoaspirate

Lipoaspirate could be cryopreserved with or without different percentage of Dimethyl Sulfoxid (DMSO) directly at -80°C or using a controlled-rate freezing container (CoolCell®). To recovery from cryopreservation the vials containing tissue were placed into a 37°C water bath for few seconds. Thawed tissue was directly seeded on the plate or pellet was seeded after centrifugation (920 x *g* for 10') with αMEM or SCM.

3.3.3 Characterization of lipoaspirated adipose tissue

Histological analyses were performed on fresh or cryopreserved lipospirate on samples coming from the same subject. Formalin-fixed paraffin-embedded tissue samples were processed for conventional histopathological examination and immunohistochemistry.

3.3.3.1 Histological characterization

Standard thick tissue sections (4 μm), stained with hematoxylin and eosin (H&E), were examined by direct wide field light microscopy.

The protocol used was the following:

1. Deparaffination with xylene for 8’ or more .
2. Rehydration:
    a. 100% ethanol for 5’.
    b. 95% ethanol for 5’.
    c. 70% ethanol for 5’.
    d. Wash two times with dH_2O for 5’ (each).
3. Coloration:
    a. Hematoxylin for 1’30’’-5’.
    b. 4-5 washes with dH_2O.
    c. Wash with H_2O.
    d. Eosin for 1’’-2’’.
    e. 4-5 washes with dH_2O.
    f. Wash with H_2O.
4. Dehydration:
    a. 95% ethanol for 5’.
    b. 100% ethanol for 5’.
5. Xilene for 8’.
6. Mount using Permount™ medium:
    a. Place a drop of Permount™ medium on the slide.
    b. Let fall gently the coverslip on the slide.
    c. Be sure that the Permount™ is covering all the tissue.
7. Dry overnight at room temperature.

3.3.3.2 Immunohistochemical characterization

A - Immunohistochemistry

Standard thick tissue sections (4 μm) were stained and immuno-reactivity was evaluated by direct wide field light microscopy.

The protocol used was the following:

1. Deparaffination with xylene for 8' or more
2. Rehydration:
    a. 100% ethanol for 5'.
    b. 95% ethanol for 5'.
    c. 70% ethanol for 5'.
    d. Wash two times with dH_2O for 5' (each).
3. Perform Sodium Citrate Antigen Retrieval as following:
    a. Place slides in a glass slide holder and fill in the rest of the rack with blank slides to ensure even heating.
    b. Place rack in 60 mL of 10 mM Sodium Citrate (pH 6.0, 100 mM) in a 500 mL glass beaker.
    c. Microwave for 20' at 700-750 watts, replacing evaporated water every 10'.
    d. Cool slides for 20' in the beaker.
    e. Wash slides three times for 5' in PBS (each).
    f. Microwave for 20', replacing evaporated water every 10'.
    g. Cool slides for 20' in the beaker.
    h. Wash three times in PBS.
4. Block aldehydic groups incubating slides with NH_4Cl 0.05 M in PBS for 30'.
5. Wash slides three times for 5' in PBS (each).

6. Quence endogenous peroxidase activity with 3% hydrogen peroxide in distilled water for 10'.
7. Wash slides three times in PBS for 5' (each).
8. Permeabilize membrane and block aspecific groups incubating slides with PBS + 1% V/V fetal bovine serum + 0.2% Triton X-100 for 1h at room temperature.
9. Wash slides three times for 5 min in PBS 0.01 M (each).
10. Incubate slides with 50-75 µL of primary antibody diluted in blocking buffer overnight at 4°C in humidified condition chamber.
11. Wash slides three times for 5' in PBS (each).
12. Dilute biotinylated secondary antibody (dilution 1:100 in blocking buffer). Add 50-75 µL per section and incubate 2-3 h at room temperature in a humid chamber.
13. Wash slides three times for 5' in PBS (each).
14. Add 1 drop of ABC kit (Pierce Biotechnology, Rockford, IL), prepared following manufacturer's instruction, to each section and incubate samples for 45' at room temperature.
15. Make 3,3-diaminobenzidine (DAB) according to the instructions in dH_2O (Pierce Biotechnology, Rockford, IL), add it immediately to slides and wait for color change (approximately 2-10').
16. Drain slides and wash with dH_2O for 5' (the slides can be left in water longer).
17. Counterstain with hematoxylin.
18. Dehydrate sections:
    a. 5' with 75% ethanol.
    b. 5' with 100% ethanol.
    c. 8' with xylene.

19. Mount using Permount™ medium:
    a. Place a drop of Permount™ medium on the slide.
    b. Let fall gently the coverslip on the slide.
    c. Be sure that the Permount™ is covering all the tissue.
20. Dry overnight at room temperature.

In control determinations, primary antibodies were omitted and replaced with equivalent concentrations of unrelated IgG of the same subclass.

Positive cells were quantified considering 50 high magnification histological fields (40X). Results were expressed as number of positive cells per histological power field (hpf).

The following primary antibodies were used:

- Anti-Vimentin (1:5000; Dako Cytomatic, Denmark).
- Anti-S100 (1: 2000; Novocastra).
- Anti-β-Tubulin III (1:6000; Covance).
- Anti-human Nestin (1:2000; Millipore).

B - Immunofluorescence

Standard thick tissue sections (4 μm) were stained and immuno-reactivity was evaluated by direct wide field light microscopy.

The protocol used was the following:

1. Deparaffination: Xylene for 10’ or more.
2. Rehydration:
    a. 100% ethanol for 5’.
    b. 95% ethanol for 5’.

c. 70% ethanol for 5'.

d. dH_2O for 5'.

e. Wash 2-3 times with PBS for 5'(each).

3. Permeabilize and block aspecific groups incubating tissue sections with 10% permeabilization solution (PB + 10% V/V BSA + 0.2% V/V Triton X-100) for 1h30' at room temperature in humidified condition chamber.
4. Wash 2 times with PBS for 5' (each).
5. Incubate slides with 200 µL of primary antibody diluted in 5% permeabilization solution (1:1, 10% permeabilization solution: PBS) overnight at 4°C in humidified condition chamber or for 1h30' at room temperature.
6. Wash 2 times with PBS for 5'.
7. Incubate slides with 200 µL of secondary antibody diluted in PBS for 2h at room temperature.
8. Wash 2 times with PBS for 5' (each).
9. Incubate the slides with 200 µL of DAPI for 10' at room temperature.
10. Wash with PBS.
11. Mount using FluorSave™ Reagent (Calbiochem, Merck Chemical, Darmstadt, Germany:
    a. Place a drop of FluorSave™ on the slide.
    b. Let fall gently the coverslip on the slide.
    c. Be sure that the FluorSave™ is covering all the tissue.
12. Dry overnight at room temperature.

Sections were analyzed by Leica SP2 confocal microscope with He/Kr and Ar lasers (Heidelberg, Germany). As negative reference for the confocal analysis we used a consecutive section that was

stained by omitting primary antibodies and replacing them with equivalent concentrations of unrelated IgG of the same subclass. The zero level was adjusted on this reference and used for all the further analyses (we used a new zero reference for each new staining). Positive cells were counted in 4 fields taken in the same section. The positive cells present in a group of three consecutive sections were averaged and we repeated this count each 100 μm. Results were expressed as percent of positive cells per histological power field (hpf). DAPI supplied the total number of cells being a nuclear staining. This quantification was performed with sections from two different patients.

The following antibodies were used:

- Primary antibodies
  - Anti-Vimentin (VIM; 1:30; Millipore).
  - Anti-Fatty Acid Binding Protein 4 (FABP4; 1:200; ; Cell Signaling Technology).
  - Anti-Neuronal Class III β-Tubulin (TUJ; monocl. 1:500; Covance, NJ, USA).
  - Anti-Glial fibrillary acidic protein (GFAP; monocl. 1:1000; Covance, NJ, USA)
- Secondary antibodies
  - Alexa Fluor 488 anti-mouse, rabbit or goat (1:1000; Invitrogen).
  - Alexa Fluor 543 anti-mouse, rabbit or goat (1:1000; Invitrogen).

3.4 ADIPOSE DERIVED STEM CELLS

3.4.1 hADSCs isolation and culture

Stem cells from lipoaspirated adipose tissue, fresh or cryopreserved were obtained either centrifuging the tissue (920 x *g* for 10') and seeding the pellet, or directly plating it without centrifugation, in

aMEM or SCM. The resulting cell populations were termed human Adipose Derived Stem Cells (hADSCs).

All cell cultures were maintained at 37°C in humidified atmosphere containing 5% CO_2. After 2 weeks, the non-adherent fraction was removed and the adherent cells were cultured continuously, while the medium was changed every 3 days. Before seeding, cell samples were tested for viability by means of Trypan blue exclusion test. To prevent spontaneous differentiation, cells were maintained at a sub-confluent culture level; therefore, when both SCM cells and αMEM cells reach 85% confluence, they were detached from the plate by 0.05% trypsin/EDTA solution, collected by centrifugation (500 x *g* for 5') and expanded in culture for many passages.

3.4.2 Culture of cryopreserved hADSCs

hADSCs were cryopreserved with 10% of Dimethyl Sulfoxid (DMSO) directly at -80°C or using a controlled-rate freezing container (CoolCell®). To recovery from cryopreservation, the vials containing the cells were placed into a 37°C water bath for few seconds. Thawed cells were then seeded on a plate in αMEM or SCM.

3.4.3 Cell Growth Analysis

Analysis was performed evaluating the proliferative capacity of hADSCs from 6 patients, maintained in culture (either in αMEM or SCM). The analyses were performed for cells at culture passage 2, fresh and cryopreserved for at least 1 month. Cells were seeded into 48-wells culture plates (Corning Life Sciences, New York, USA) and maintained in culture in aMEM and SCM. Live cells were counted by Trypan blue exclusion at 85% confluence. Cell doubling times (DT) and numbers (CD) were calculated with haemocytometer counts (Neubauer Chamber) (VWR International Radnor, Pennsylvania, USA) and cell culture time (CT) for each passage by the following formula: CD= ln(Nf/Ni)/ln2 and

DT=CT/CD, where DT is the cell doubling time, CT the culture time, CD the cell doubling number, Nf the final number of cells, and Ni the initial number of cells.

The experiments were performed at least three times for each point reported in the curve.

3.4.4 Flow cytofluorimetry - Immunophenotypic characterization

Cultures of hADSCs at different passages were phenotypically characterized by Fluorescence-Activated Cell Sorting (FACS), using the following protocol:

1. After trypsinization, centrifuge (500 x *g* for 5') and count.
2. Re-suspend $1x10^5$ cells in 250 µL PBS w/o Ca^{2+} and Mg^{+} (Euroclone Italy).
3. Add primary antibodies pipetting few times.
4. Vortex and keep the samples for 30' out of light at 4°C.
5. Add 1ml of PBS and centrifuge (500x *g* for 10').
6. Leave 250 µL of supernatant in the tubes and re-suspend the pellet.
7. Add 250 µL of 4% PFA.
8. Set the instrument and analyze by flow cytometry (FACS Vantage, BD Bioscience) using a specific software (CellQuest Pro, BD Bioscience).

The following antibodies were used:

- anti-CD44 (BD Biosciences, Italy).
- anti-CD90 (Millipore, Italy).
- anti-CD34 (Mylteni Biotec, Italy).
- anti-CD45 (BD Biosciences, Italy).
- anti-CD146 (Biocytex, USA).
- anti-CD31 (Mylteni Biotec, Italy).
- anti-CD56 (Mylteni Biotec, Italy).

- anti-CD105 (Serotec, USA).
- anti-CD144 (R&D System, USA).
- anti-CD133 (Mylteni Biotec, Italy).
- KDR (R&D System, USA).
- CD73 (BD Biosciences, Italy).
- anti-CD166 (BD Biosciences, Italy).

3.4.5 Immunocytochemical analysis: Immunofluorescence

hADSCs obtained from adipose tissue were seeded (3.5 x 10^3 cells/cm^2) on glass slides and were stained by indirect immunofluorescence at 85% confluence, using the following protocol:

1. Fix cells:
    a. Remove medium and wash with PBS.
    b. Add 2% PFA for 15'.
    c. Wash with PBS for 10'.
    d. Wash with PBS for 5'.
2. Add 200 µL of 4% saturation solution (4% BSA, 0.3% Triton X-100 in PBS) for 20'
3. Remove and add 200 µL of 0.4% saturation solution (0.4% BSA, 0.03% Triton X-100 in PBS) for 10'.
4. Remove and 100 µL of primary antibody for 1h30' at room temperature or overnight at 4°C in humidified condition chamber.
5. Remove and wash 3 times with PBS for 10' (each).
6. Add 100 µL of secondary antibody diluted in 0.4% saturation solution for 45' out of light.
7. Wash with 500 µL of 0.4% saturation solution for 15'.
8. Wash 3 times with PBS for 10' (each).

9. Remove and add 80 µL of Hoechst (0.02 µg/µL in PBS, Invitrogen).
10. Remove Hoechst and wash 2 times with PBS.
11. Mount using FluorSave™ Reagent (Calbiochem, Merck Chemical, Darmstadt, Germany):
    a. Place a drop of FluorSave™ on the microscope slide.
    b. Let fall gently the glass coverslip with the cells on the side of the slide.
    c. Keep attention to not make bubbles.
12. Dry overnight at room temperature.

The following antibodies were used:

- Primary antibodies

- Anti-Vimentin (VIM; 1:30; Millipore).
- Anti-Neuronal Class III β-Tubulin (TUJ; monocl. 1:500; Covance, NJ, USA).
- Anti-Microtubule-associated protein 2 (MAP2; monocl. 1:200; Sigma-Aldrich).
- Anti-human Nestin (monocl.1:100; R&D Systems).
- Anti-Glial fibrillary acidic protein (GFAP; monocl. 1:1000; Covance, NJ, USA).
- Anti-Oligodendrocyte marker (O4; monocl. 1:150; Chemicon).

- Secondary antibodies

- Alexa Fluor 488 anti-mouse, rabbit or goat (Invitrogen).
- Alexa Fluor 543 anti-mouse, rabbit or goat (Invitrogen).

Images were taken using Leica SP2 confocal microscope with He/Kr and Ar lasers (Heidelberg, Germany). In negative control experiments, primary antibodies were replaced with equivalent concentrations of unrelated IgG of the same subclass. The quantification of positive cells was

performed by considering on a minimum of 9 independent fields (3 fields/3 coverslips/treatment) of photomicrographs captured with 20X objective. Total count of each markers immunoreactive cells was performed and the number of positive cells expressed as the percentage to the total cells. DAPI supplied the total number of cells being a nuclear staining.

3.4.6 In vitro differentiation

A - Adipogenic differentiation

hADSCs, grown in αMEM or SCM, were seeded ($6x10^3$ cells/cm^2) in adipogenic medium following already published protocols [55]. Adipogenic medium consisted of DMEM supplemented with 10% FBS, 1 μM dexamethasone, 0.5 mM 3-isobutyl-1-methyl-xanthine, 10 μM insulin and 200 μM indomethacin. After two weeks in culture cells were fixed and stained using the following protocol:

1. Remove most of the medium.
2. Add 10% formalin in incubate 5' at room temperature.
3. Discard formalin and add the same volume of fresh formalin. Incubate at least 1 h or longer.
4. Remove all the formalin and wash wells with PBS.
5. Remove and wash wells with 60% isopropanol 40% dH_2O for 5'.
6. Let the wells dry completely.
7. Add 800 μL of Oil Red O working solution for 15' (do not touch walls of the wells).
8. Remove all Oil Red O and IMMEDIATELY add dH_2O.
9. Wash 4 times with H_2O.
10. Take pictures if desired.
11. Remove all water and let dry.

12. Elute Oil Red O by adding 100% isopropanol, incubate about 10' (can be longer).
13. Pipet the isopropanol with Oil Red O up and down several times to be sure that all Oil Red O is in the solution.
14. Transfer to 1.5 mL tubes -Measure OD at 500 nm, 0.5'' reading.
15. As blank use 100% isopropanol. As control use isopropanol from empty well stained as previously described.

Another protocol to stain mature adipocytes was used by means of FABP4 staining with the Human Mesenchymal Stem Cell Functional Identification Kit (R&D Mesenchymal Stem Cells, according to manufacturer instructions.

B - Osteogenic differentiation

hADSCs, grown in αMEM or SCM, were seeded ($9.5x10^3$ cells/cm^2) in osteogenic medium containing DMEM Low Glucose, 10% FBS, 10 nM dexamethasone, 200 μM ascorbic acid (Sigma-Aldrich St. Louis, MO, USA), 10 mM β-glycerol phosphate (Sigma-Aldrich St. Louis, MO, USA). After three weeks in culture, cells were fixed and stained using the following protocol:

1. Wash 2 times in PBS for 5' (each).
2. Fix in EtOH 70% for 10'.
3. Wash 2 times in PBS for 5'.
4. Add Alizarin Red S dye (Sigma-Aldrich St. Louis, MO, USA, 1mg/mL in dH_2O, pH 7.55) for 30'-1h.
5. Wash in H_2O.

Intracellular alkaline phosphatase (ALP) activity was measured colorimetrically using an Alkaline Phosphatase Colorimetric Assay Kit (Abcam, Cambridge, UK), which uses p-nitrophenyl phosphate (pNPP) as a phosphatase substrate that turns yellow (λ_{max}= 405 nm) when dephosphorylated by ALP.

1. Prepare cell lysate using three cycles of freeze-thaw in deionized distilled water.
2. Add 30 µL of the cell lysate to a 96 wells plate with 50 µL Assay buffer.
3. Use a sample background control. Add the same amount of sample into separate wells, bring volume to 80 µL. Add 20 µL stop solution and mix well to terminate ALP activity in the sample.
4. Add 50 µL of the 5 mM pNPP solution to each well containing the test samples and background controls and mix well.
5. Incubate the reaction for 60' at 25°C, protect from light.
6. Stop all reactions by adding 20 µL Stop Solution into each standard and sample reaction except for the sample background control reaction and gently shake the plate.
7. Measure OD at 405 nm in a microplate reader (Programmable MPT Reader, Giorgio De Vita).

<u>To prepare the Standard Curve</u>:

1. Dilute 40 µL of the 5 mM pNPP solution with 160 µL Assay Buffer to generate 1 mM pNPP standard.
2. Add 0, 4, 8, 12, 16, 20 µL into 96-well plate in duplicate to generate 0, 4, 8, 12, 16, 20 nmol/well pNPP standard. Bring the final volume to 120 µL with Assay Buffer.

3. Add 10 µL of ALP enzyme solution to each well containing the pNPP standard and mix well. The ALP enzyme will convert pNPP substrate to an equal amount of colored p-Nitrophenol (pNP).
4. Incubate the reaction for 60’ at 25°C, protect from light.

Another protocol to stain mature osteocytes was used by means of Osteocalcin staining with the Human Mesenchymal Stem Cell Functional Identification Kit (R&D Mesenchymal Stem Cells, according to manufacturer instructions.

3.5 CONFOCAL MICROSCOPY

Confocal microscopy offers several advantages over conventional optical microscopy, including controllable depth of field, the elimination of image degrading out-of-focus information, and the ability to collect serial optical sections from thick specimens. The key to the confocal approach is the use of spatial filtering to eliminate out-of-focus light or flare in specimens that are thicker than the plane of focus. In recent years, there has been a tremendous explosion in the popularity of confocal microscopy, due in part to the relative ease with which extremely high-quality images can be obtained from specimens prepared for conventional optical microscopy.

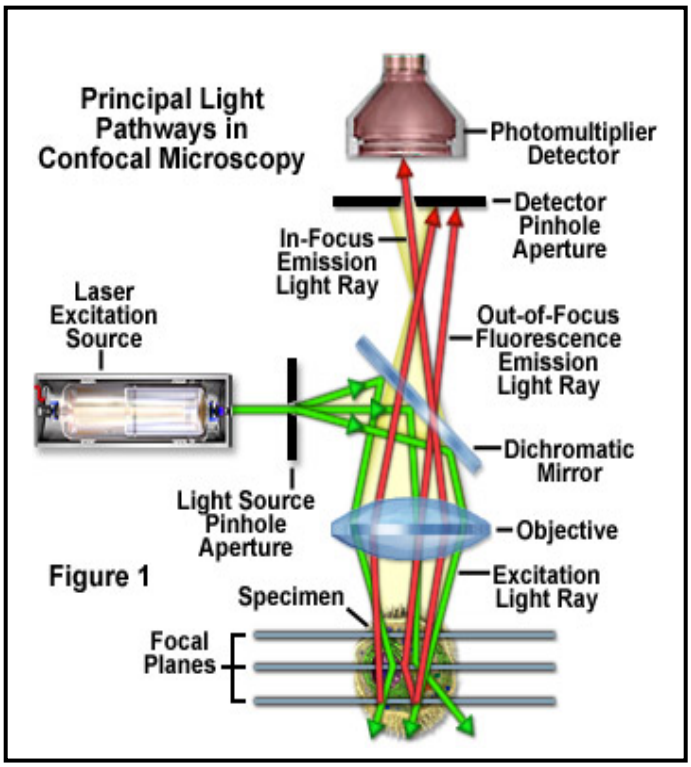

Figure 4: Scheme of confocal microscopy.

In a conventional wide field microscope, the entire specimen is bathed in light from a mercury or xenon source, and the image can be viewed directly by eye or projected onto an image capture device or photographic film. In contrast, the method of image formation in a confocal microscope is fundamentally different. Illumination is achieved by scanning one or more focused beams of light, usually from a laser or arc-discharge source, across the specimen. This point of illumination is brought to focus in the specimen by the objective lens, and laterally scanned using some form of scanning device under computer control. The sequences of points of light from the specimen are detected by a photomultiplier tube (PMT) through a pinhole (or in some cases, a slit), and the output from the PMT is built into an image and displayed by the computer. Although unstained specimens can be viewed using light reflected back from the specimen, they usually are labeled with one or more fluorescent probes.

3.5.1 Specimen Preparation and Imaging

The procedures for preparing and imaging specimens in the confocal microscope are largely derived from those that have been developed over many years for use with the conventional wide field microscope. In the biomedical sciences, a major application of confocal microscopy involves imaging either fixed or living cells and tissues that have usually been labeled with one or more fluorescent probes. A large number of fluorescent probes are available that, when incorporated in relatively simple protocols, specifically stain certain cellular organelles and structures. Among the plethora of available probes are dyes that label nuclei, the Golgi apparatus, the endoplasmic reticulum, and mitochondria, and also dyes such as fluorescently labeled phalloidins that target polymerized actin in cells. Regardless of the specimen preparation protocol employed, a primary benefit of the way in which confocal microscopy is carried out is the flexibility in image display and analysis that results from the simultaneous collection of multiple images, in digital form, into a computer.

3.5.2 Critical aspects of Confocal microscopy

Quantitative three-dimensional imaging in fluorescence microscopy is often complicated by artifacts due to specimen preparation (*e.g.* autofluorescence problems, retractile structures presence, presence or absence of highly stained structures, immersion oil, coverslip thickness etc.), controllable and uncontrollable experimental variables or configuration problems with the microscope (*e.g.* optical component alignment, objective magnification, bleaching artifacts, aberrations, quantum efficiency, and the specimen embedding medium).

In our experimental conditions, the immunofluorescence experiments were assessed by confocal microscopy TSC SP2 Leica.

4 RESULTS

Following our previous experience with mesenchymal stem cells characterization [66] [67], we have developed a set of methods for the characterization of Human Olfactory Ensheathing Stem Cells from superior turbinate tissue and for the characterization of human Adipose Derived Stem Cells from lipoaspirate tissue.

4.1 Isolation and characterization of human adipose derived stem cells (hADSCs)

4.1.1 Immunohistochemical features of lipoaspirate

Paraffin embedded sections of lipoaspirate were studied by immunohistochemistry. The expression of vimentin, nestin, and β-tubulin III was investigated in fresh (**Figure 5 A**) and cryopreserved tissue (**Figure 5 B**) as well as in cell pellet from fresh tissue (**Figure 5 C**). In the fresh tissue, the quantification of the specific nestin positive cells distribution was 0.95% ± 0.03 positive cells/hpf (histological power field), vimentin stained 98,8% ± 0,9 of the cells, whereas staining for β-tubulin III was negative. These data were confirmed in the cryopreserved tissue and pellet. The S100 expression (a glial marker in the peripheral tissues) was 0.97% ± 0.02 in the investigated fresh tissue. Hematoxylin and eosin showed the tissue structure.

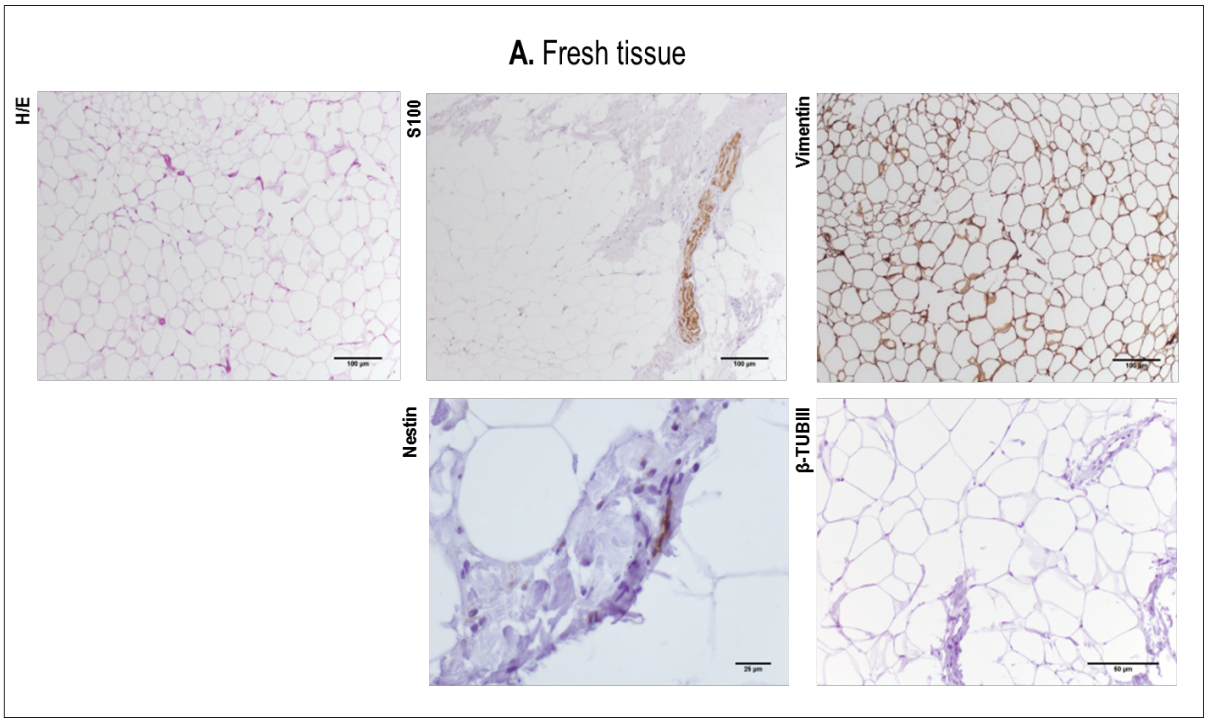

Fresh lipoaspirated tissue	vimentin	nestin	S100	β-tubulin III
% of positive cells/hpf ± SEM	98,8 % ± 0,9	0.95 % ± 0.03	0.97 % ± 0.02	none

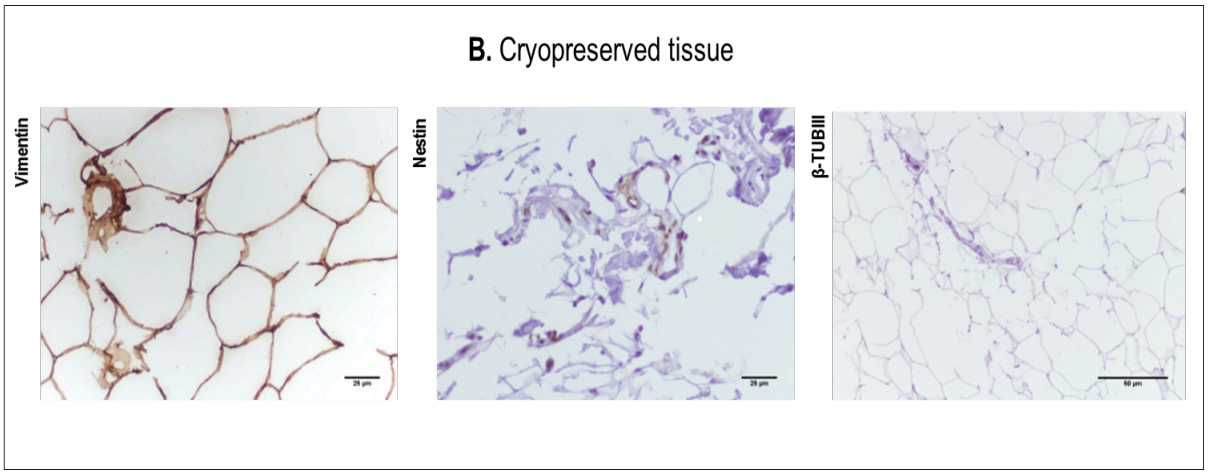

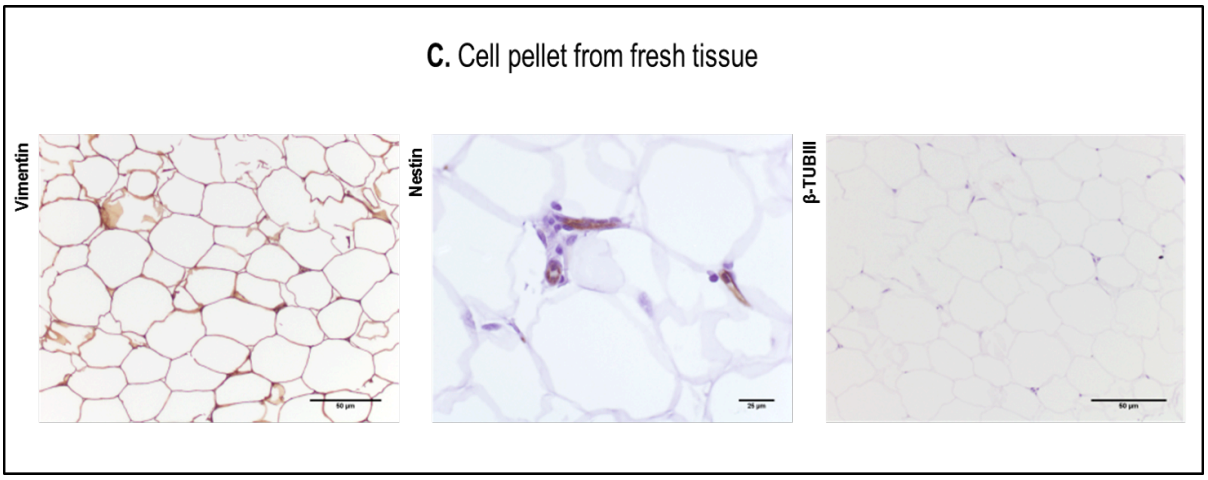

***Figure 5**: **Histology and immunohistochemistry of lipoaspirated adipose tissue**. (A) Immunohistochemical analyses were performed on fresh tissues. Quantification is expressed as % of positive cells/hpf (B) after their cryopreservation at -80° for 72 hours and (C) on the pellet of cells obtained after the fresh tissues centrifugation). The pictures shown were obtained from one patient and are representative of the other investigated cases (n=3).*

To confirm and examine in depth the immunohistichemical features of the tissue, we also performed an immunofluorescence analysis. Confocal analysis appeared to be more efficient in revealing positive cells, in fact β-tubulin III positive cells were found (**Figure 6 A**). Positive GFAP cells were also identified in the tissue (**Figure 6 C**). As general markers of adipose tissue, we have followed fatty acid binding protein 4 (FABP4), and vimentin as a mesenchymal marker (**Figure 6 B and D**).

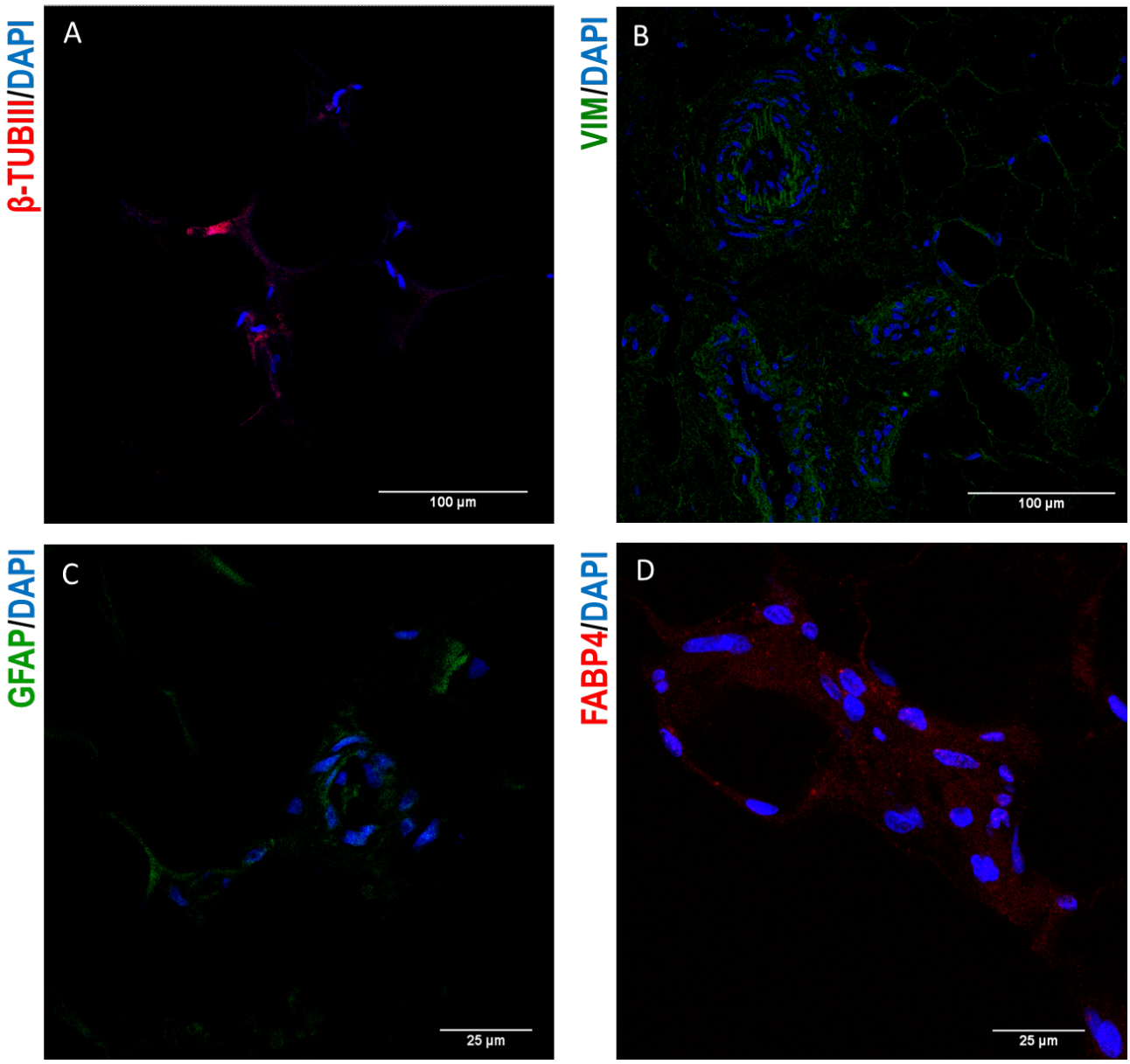

	β-tubulin III	Vimentin	GFAP	FABP4
% of positive cells	9.7 % ± 1.2	98,9 % ± 0.91	58.1% ± 5.6	96.3 % ± 3.52

Figure 6: Tissue markers expression. *The expression β-tubulin III, vimentin, fatty acid binding protein 4 (FABP4) and GFAP were investigated by immunofluorescence. The pictures shown were obtained from one patient and are representative of the other investigated 3 cases. Scale bars are 100 µm in panels A, B and 25 µm in panels C, D.. Quantification is expressed as mean of positive cells ± SEM.*

4.1.2 Proliferative features of lipoaspirate-derived hADSCs

Expansion curves of cell populations obtained from different patients (**Figure 7 A**) were established in order to investigate the growth capability of purified hADSC. The number of hADSCs doublings in culture was comparable among the different cases at the same time points. Similar data were previously reported by other authors [68]. No differences in growth curves were observed when hADSCs were cultured after cryopreservation, using the two media (**Figure 7 B**).

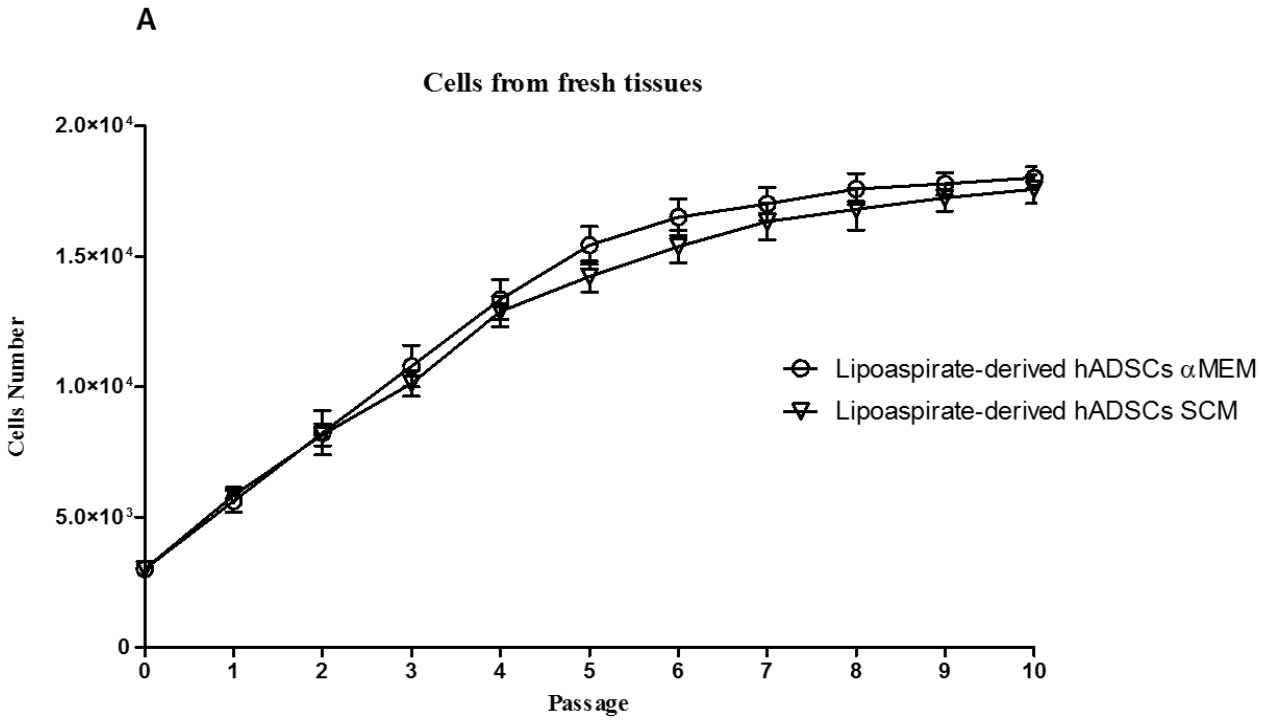

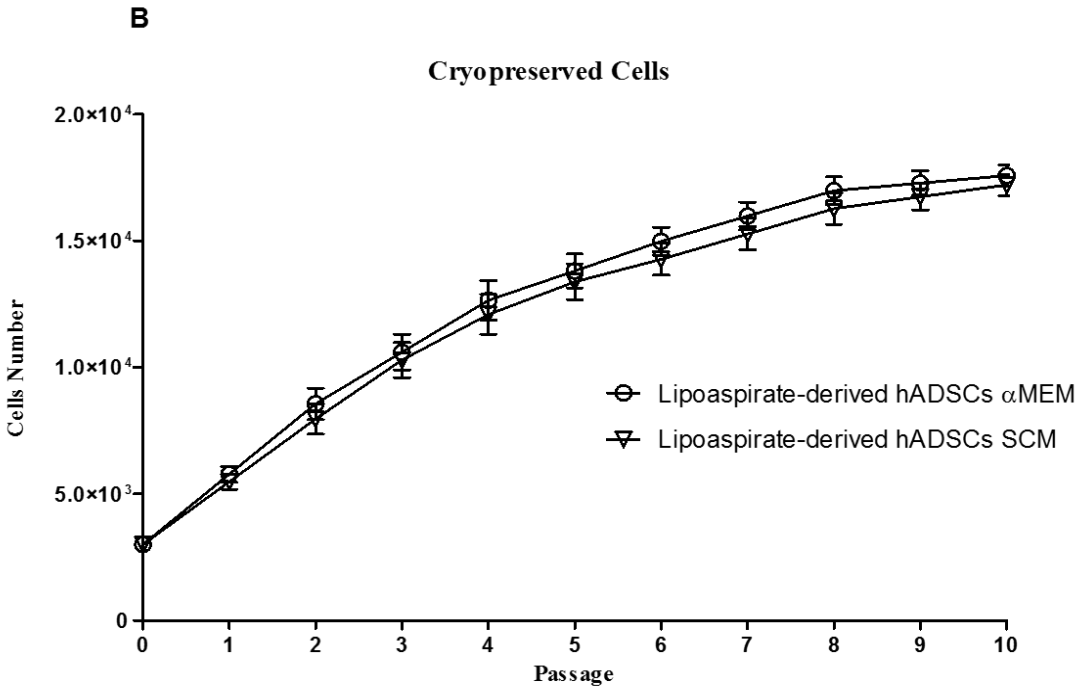

Figure 7: Expansion curves of hADSCs. *Each point of the growth curves represent the mean ± SEM of counts for cells obtained from 6 cases, for the first 10 passages. (A) Cells were obtained from fresh tissue and (B) cells obtained from fresh tissue and then cryopreserved.*

4.1.3 Flow cytofluorimetry detection of mesenchymal hADSCs surface markers

Although many efforts had been made toward the characterization of surface markers of mesenchymal stem cells, a specific marker, capable of identifying an uniquely homogeneous mesenchymal cell population, is not yet identified. Many useful phenotypic profiles for the study of cell-cell interactions and cell-environment are however well known [69]. hADSCs, purified from three different subjects at passage 2, randomly chosen and grown αMEM medium at 90% confluence, were studied by means of FACS analyses. These data highlight that the expression of surface markers molecules was very similar in hADSCs samples obtained from different individuals. hADSCs express high values of known mesenchymal markers (such as CD44, CD73, CD90, CD105 and CD166). As expected, endothelial (CD31, CD34, CD144, CD146, KDR) and hematopoietic (CD45, CD133) markers were less represented (**Figure 8***)*.

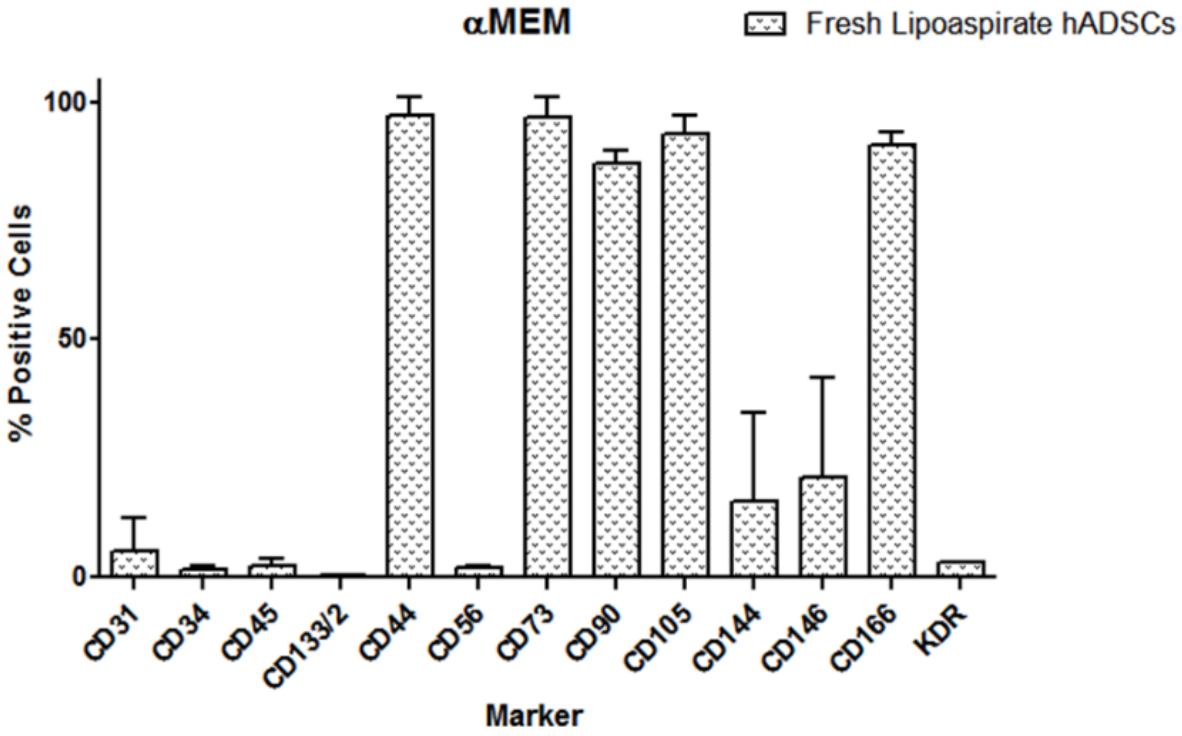

Figure 8: Cell surface phenotype of lipoaspirate derived hADSCs. *Cell surface phenotype was investigated by FACS on hADSCs obtained from lipoaspirated adipose tissue maintained in αMEM at early passage (passage 2). The assay was performed in three different cases, each case was investigated in triplicate.*

Markers list	
CD31	Platelet endothelial cell adhesion molecule (PECAM-1); CD34: It may also mediate the attachment of stem cells to bone marrow extracellular matrix or directly to stromal cells.
CD34	are normally found in the umbilical cord and bone marrow as hematopoietic cells, a subset of mesenchymal stem cells, endothelial progenitor cells, endothelial cells of blood vessels but not lymphatics.
CD45	is a type I transmembrane protein that is in various forms present on all differentiated hematopoietic cells.
CD133/2	is a transmembrane glycoprotein and is expressed in hematopoietic stem cells, endothelial progenitor cells, glioblastoma, neuronal and glial stem cells.

CD44	is a cell-surface glycoprotein involved in cell–cell interactions, cell adhesion and migration. It functions as a "bone homing receptor", directing migration of human hematopoietic stem cells and mesenchymal stem cells to bone marrow.
CD56	Neural Cell Adhesion Molecule (NCAM).
CD73	is used as a marker of lymphocyte differentiation.
CD90	orThy-1: is use as a marker for a variety of stem cells and for the axonal processes of mature neurons.
CD105	It has been found on endothelial cells, activated macrophages, fibroblasts, and smooth muscle cells.
CD144	Functioning as a classic cadherin by imparting to cells the ability to adhere in a homophilic manner, the protein may play an important role in endothelial cell biology through control of the cohesion and organization of the intercellular junctions.
CD146	also known as the melanoma cell adhesion molecule (MCAM),is a cell adhesion molecule currently used as a marker for endothelial cell lineage.
CD166	hematopoietic cell antigen, also known as activated leukocyte cell adhesion molecule (ALCAM).
KDR	kinase insert domain receptor per VEGF.

Table 2: List of used FACS markers

4.1.4 In Vitro differentiation of hADSCs

4.1.4.1 Adipogenic differentiation

hADSCs, previously grown in αMEM and SCM, were seeded ($6x10^3$ cells/cm^2) in the adipogenic medium. After two weeks in culture, cells were fixed in 10% formaldehyde for 1 hour and stained with Oil red-O solution to show lipid droplets accumulation (**Figure 9 A**). For the quantification of intracellular lipid accumulation of Oil Red O, the stained lipid droplets were eluted with 100% isopropanol for 10 minutes. The optical density was measured at 500 nm by spectrophotometer [70][71]. hADSCs had an absorbance of 0.53±0.019 in αMEM and a comparable absorbance of 0.48±0.035 nm in SCM (**Figure 9 B**).

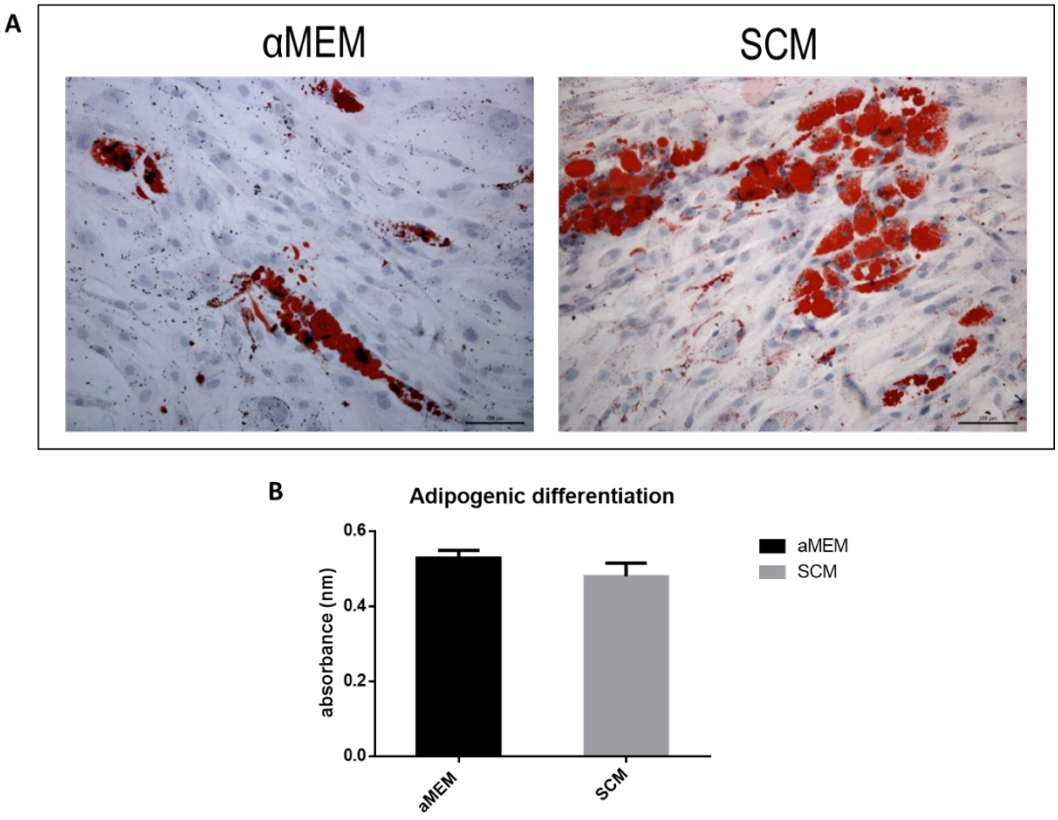

Figure 9 A-B: In vitro differentiation capability of hADSCs. *(A) Cells were in vitro differentiated. Adipogenesis was revealed by Oil Red O staining for lipid droplets. Scale Bars are 100 μm. Data are representative of two different experiments for four cases. (B) Quantification of optical density measured at 500 nm by spectrophotometer.*

The same differentiation procedure was replicated in two cases grown in αMEM and, after two weeks in culture, cells were fixed in 10% formaldehyde for 1 hour and stained for the expression of FABP4, an active adipocyte marker, by immunocytochemical methods. Fatty acid binding protein 4, FABP4, is a carrier protein for fatty acids primarily expressed in mature adipocytes. The expression of this protein in hADSCs was upregulated by the differentiation protocol (**Figure 9 D**) compared to the control hADSCs (**Figure 9 C**).

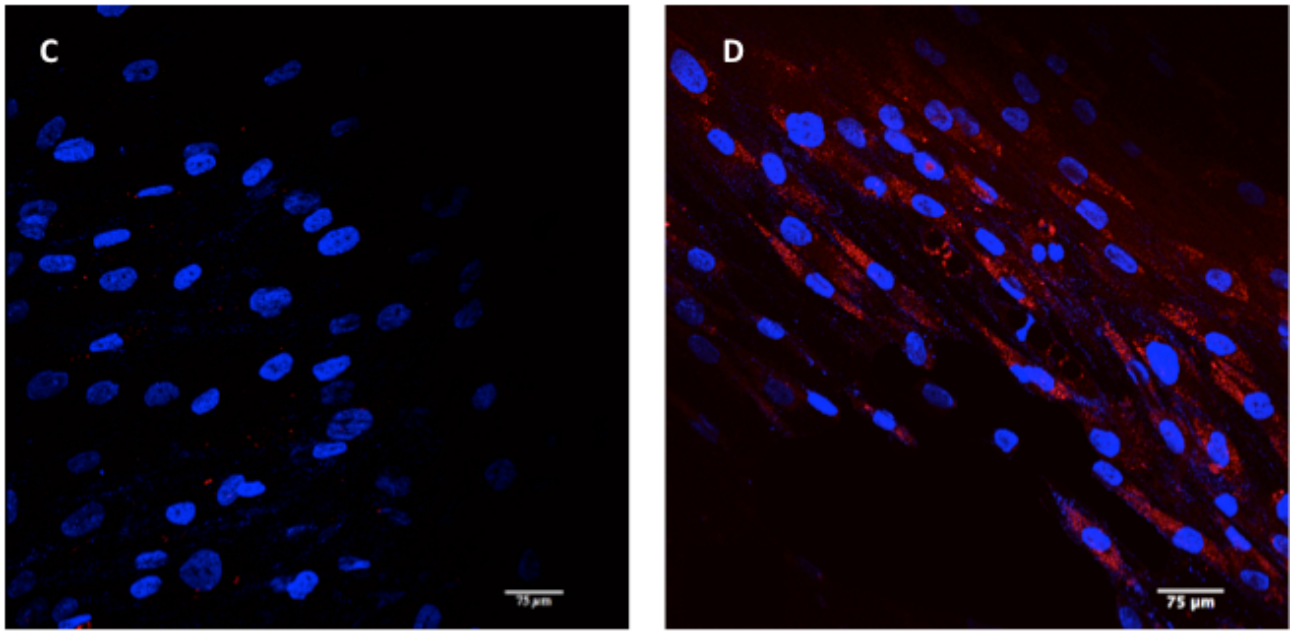

Figure 9 C-D: In vitro differentiation capability of hADSCs*. (D) Cells were in vitro differentiated. Mature adipocytes were revealed by immunofluorescence FABP4 staining. (C) non differentiated hADSCs Control. Data are representative of two different experiments for three cases. Scale Bars are 75 µm.*

4.1.4.2 Osteogenic differentiation

hADSCs, previously grown in αMEM and SCM, were seeded ($9.5x10^3$ cells/cm^2) in the osteogenic medium. Cells were maintained in culture for 3 weeks and then fixed in 70% ethanol and stained with 1mg/ml Alizarin Red S dye to detect mineralized matrix [72] (**Figure 10 A**).

Intracellular alkaline phosphatase (ALP) activity was measured colorimetrically using an Alkaline Phosphatase Colorimetric Assay Kit that uses p-nitrophenyl phosphate (pNPP) as a phosphatase substrate. Plate was read at 405 nm in a micro-plate reader (Programmable MPT Reader, Giorgio De Vita) [72]. Quantitative assay of intracellular alkaline phosphatase (AP) activity revealed that AP activity in hADSCs was comparable reaching a value of 0.15 ± 0.04 µmol/l in αMEM and of 0.14 ± 0.02 µmol/l in SCM (**Figure 10 B**).

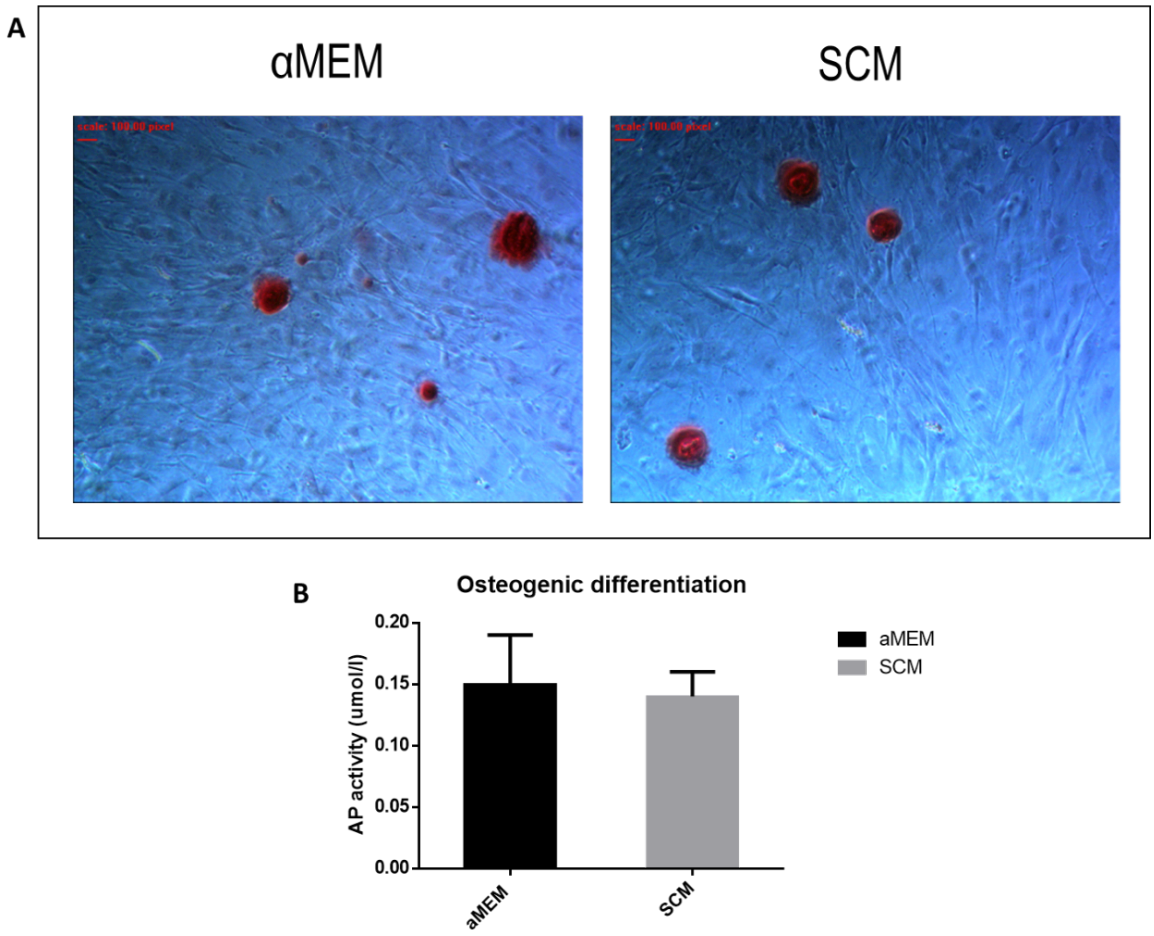

Figure 10: In vitro differentiation capability of hADSCs. *(A) Cells were in vitro differentiated. Osteogenic differentiation was evidenced by the formation of mineralized matrix as shown by Alizarin Red staining. Scale Bars are 100 pixel. Data are representative of two different experiments for four cases. (B) Quantification of AP activity measured at 500 nm by spectrophotometer.*

The same differentiation procedure was replicated in two cases grown in αMEM and, after 3 weeks, cells were fixed in 70% ethanol and stained for the expression of Osteocalcin, a biomarker of bone formation process, by immunocytochemical methods. Osteocalcin is a noncollagenous protein found in bone and thought to be pro-osteoblastic and bone-building. The expression of this protein in hADSCs was upregulated by the differentiation protocol (**Figure 10 D**) compared to the control hADSCs (**Figure 10 C**).

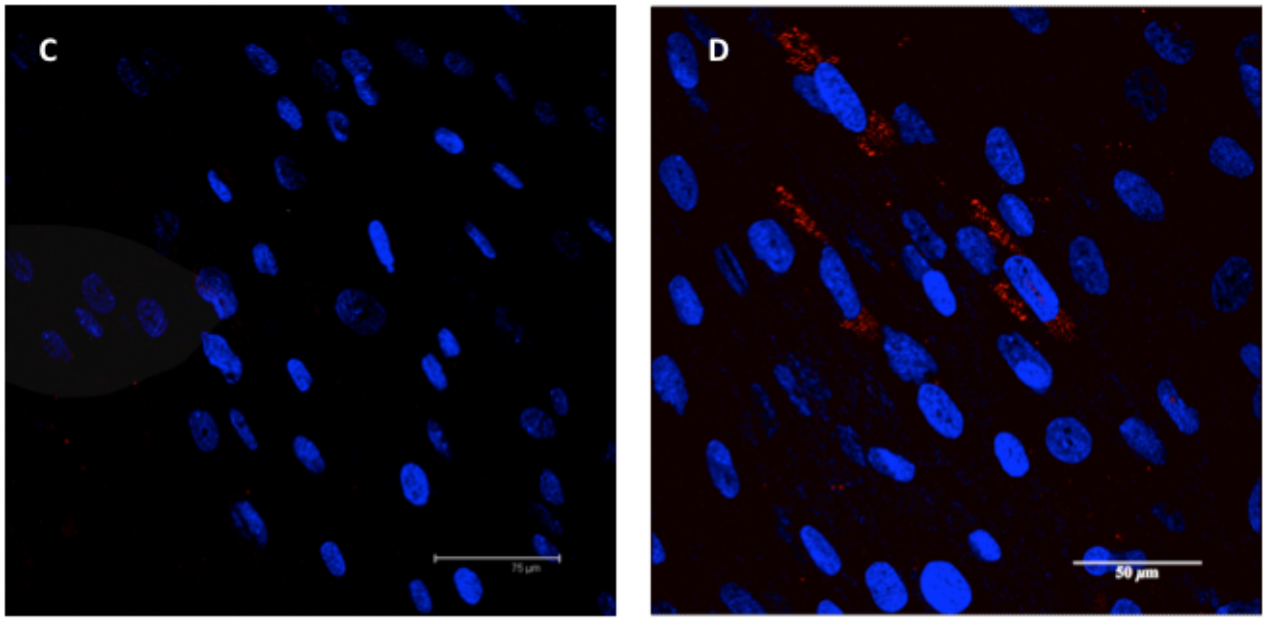

Figure 10 C-D: In vitro differentiation capability of hADSCs*. (D) Cells were in vitro differentiated towards osteogenic lineage. hADSCs expressing osteocalcin were revealed by immunofluorescence staining. (C) non differentiated hADSCs Control. Data are representative of two different experiments for three cases. Scale Bars are respectively 75 µm and 50 µm.*

4.1.5 Neural markers expression in hADSCs

To implement the characterization of hADSCs, the expression of cellular markers was evaluated by immunocytochemical methods. About 90% of cells expressed vimentin, a mesenchymal marker, and 65% of them expressed nestin, a stem cells marker. We observed a positive staining also for neural markers, such as TUJ1 (neuron – specific class III beta tubulin) and GFAP (glial fibrillary acid protein) (**Figure 11 A and B**). Similar results were achieved when immunocytochemistry was performed in hADSCs obtained from cryopreserved tissue. As shown by other authors, a reduced percentage of cells capable of expressing NG_2 and MAP2 were observed [73][74] (**Figure 11 A and B**).

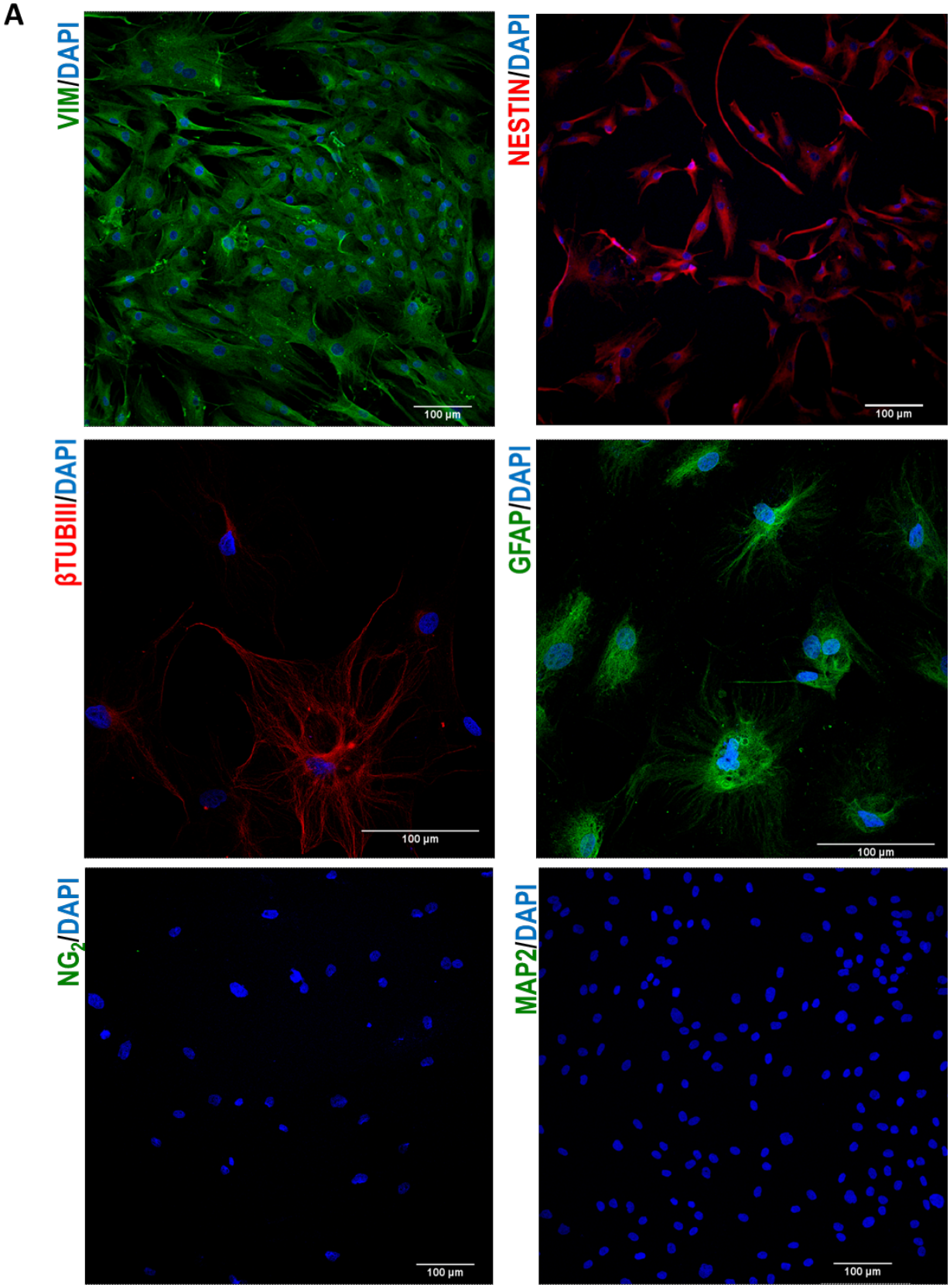
A
VIM/DAPI
NESTIN/DAPI
βTUBIII/DAPI
GFAP/DAPI
NG2/DAPI
MAP2/DAPI
100 µm

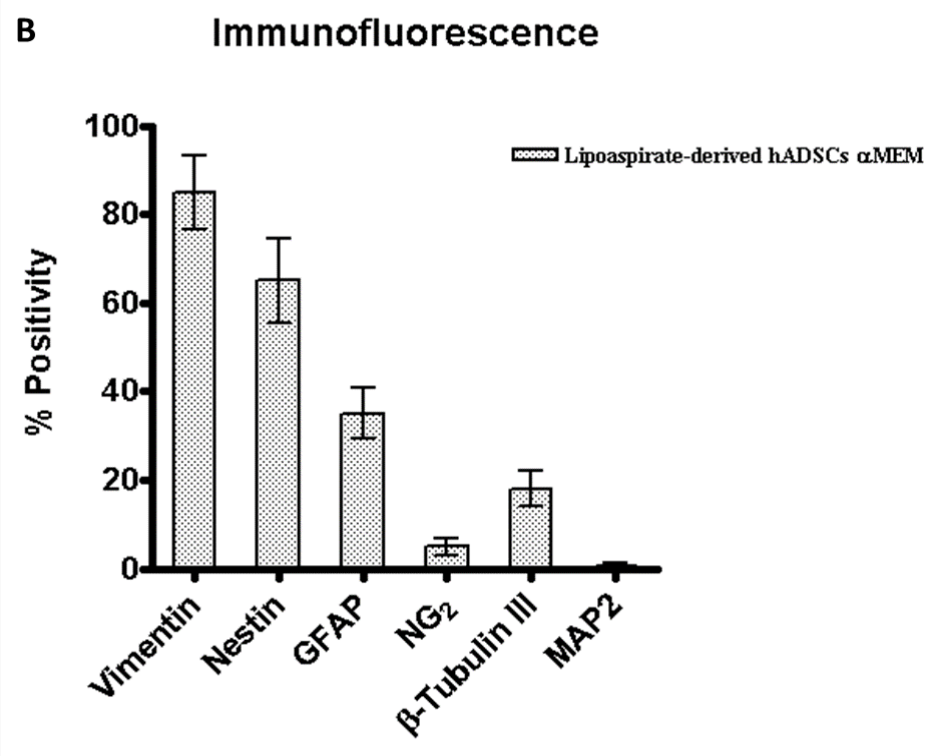

Figure 11: hADSCs markers expression. *(A) The expression of neural (β-tubulin III, GFAP, NG_2, MAP2), stem (nestin) and mesenchymal (vimentin) markers was investigated by immunofluorescence from the same case. (B) Quantification was performed by counting the number of cells positive for the staining. Positivity was expressed as a percent of the total cells. Data are expressed as the mean of three independent experiments for each case (n=9) with similar results ± SEM. Scale bars are 100 μm.*

4.2 Isolation and characterization of human olfactory Ensheathing stem cells (hOESCs)

4.2.1 Isolation and culture of Human Superior turbinate tissue-derived stem cells

Superior turbinate tissue was obtained from 9 donors who planned to undergo septoplasty, rhinoplasty and/or functional endoscopic sinus surgery. The mucosa and *lamina propria* from the posterosuperior septum or the superior nasal concha was cultured as reported in Materials and Methods.

Live morphology (captured by means of EVOS® microscope apparatus, AMG, USA) of observed cells at passage zero (48 hours after seeding, **Figure 12 A**, and at confluence, **Figure 12 B**) presented a fibroblast-like phenotype, comparable to that of hADSCs, and all samples were able to grow and proliferate in classical culture medium (TCM). The same morphology was maintained even at higher passages (passage 14).

After one to three days in culture, isolated sections of tissue and individual cells began to adhere to and grow on the bottom of the culture flask. A few days after biopsy and dissociation, cells typically began to grow and migrate outwards from the large pieces of tissue (explants) that remained after the dissociation procedure (**Figure 12 A**). The cells growing from the explants typically grew to confluence within three weeks (**Figure 12 B**), after which they were diluted to 30% density. After the initial passage, cells grew to confluence usually within a week.

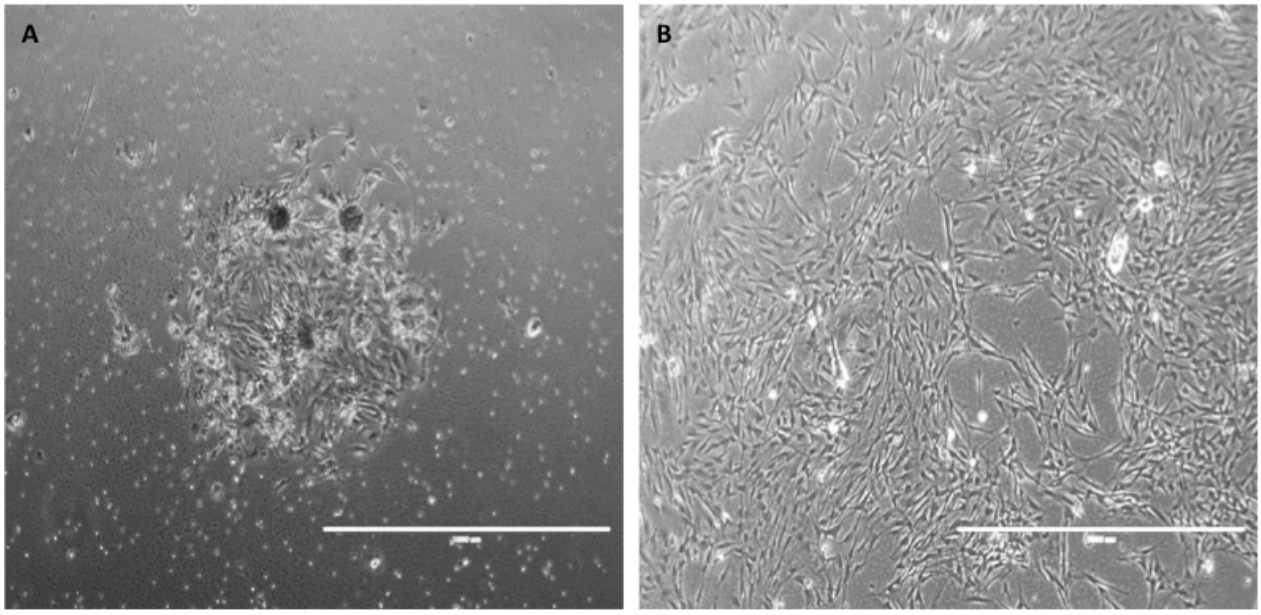

Figure 12. hOESCs at passage 0. *Morphological appearance in direct light of isolated hOESCs 48 hours after seeding (A) and at confluence (B). Scale bars are 1000 µm.*

4.2.2 Proliferative features and growth kinetics of hOESCs

In order to investigate the growth capability of hOESCs expansion curves of cell populations obtained from different patients were established. They grew slowly for the very first passages, and then entered a phase of exponential growth (around the fifth passage) (**Figure 13**). The CD was calculated in the exponential phase at passage seven, where the Doubling Time value was 5.36 ± 0.73 days.

No differences in growth curves were observed when hOESCs were cultured after cryopreservation.

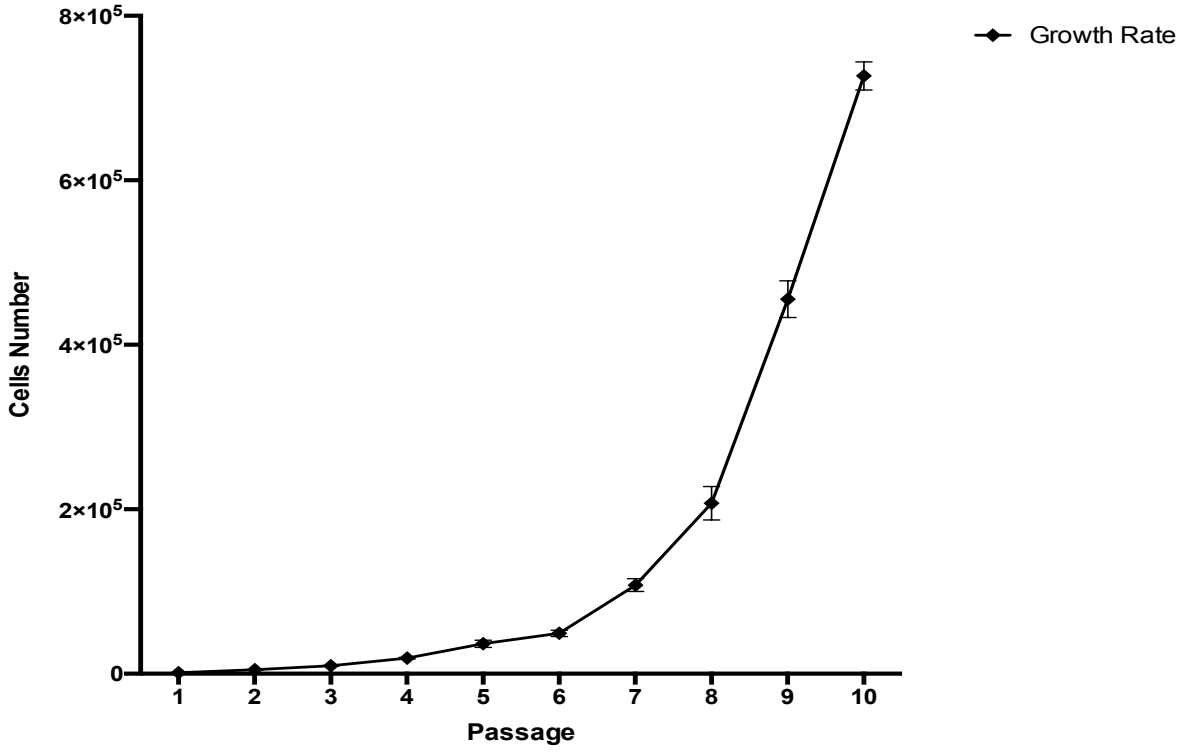

Figure 13 **Exponential curve of hOESCs grown**

4.2.3 Cell cycle and chromosomal stability

The DNA content was analyzed by Cytomics FC 500 and the cell cycle was analyzed with Cell Quest software (BD Bioscience). The results show that 18.4 ± 3.3% of hOESCs cultured in TCM were in S+G2/M (active proliferative phase) and that 81.5 ± 3.2% were in G0/G1 phase (quiescent phase).

These results do not change through a consistent number of passages (**Figure 14 A**) for all the analyzed samples (n = 4). Our results demonstrated that less than 0,6% of hOESCs grown in TCM were in apoptosis. Moreover, hOESCs did not present any chromosomal rearrangement, as assessed by QFQ-banding performed at early and late passages (**Figure 14 B**). Chromosome number was normal in all analyzed samples (n=4)

A

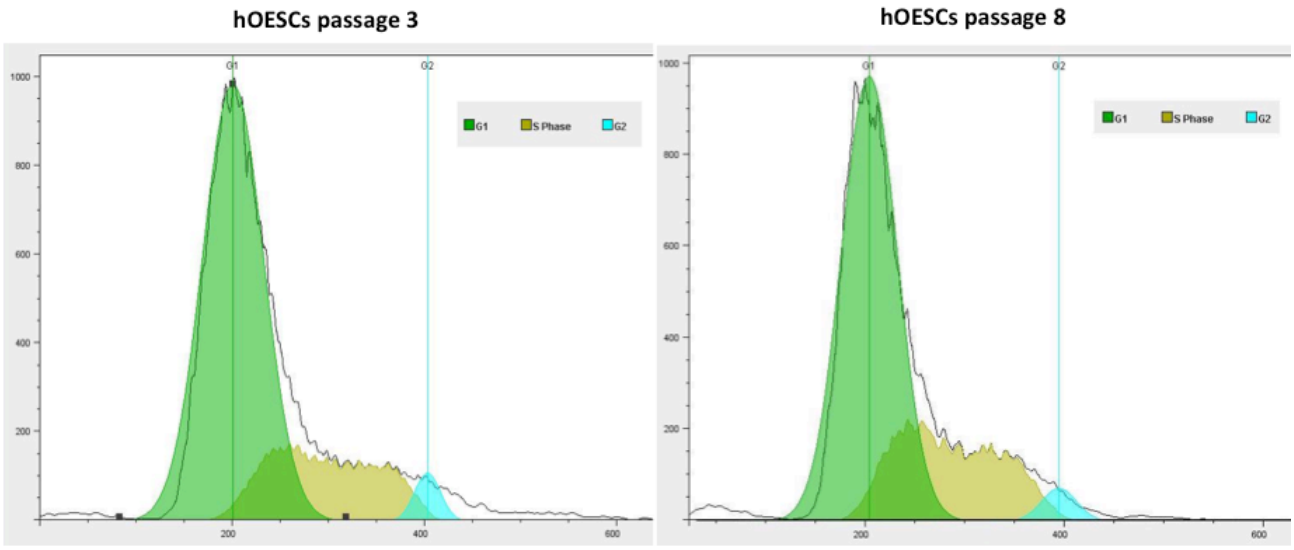

Apoptosis	0.47 ± 0.12 %
G0/G1	81.5 ± 3.2 %
S	15.5 ± 2.9 %
G2-M	2.9 ± 0.4 %

B

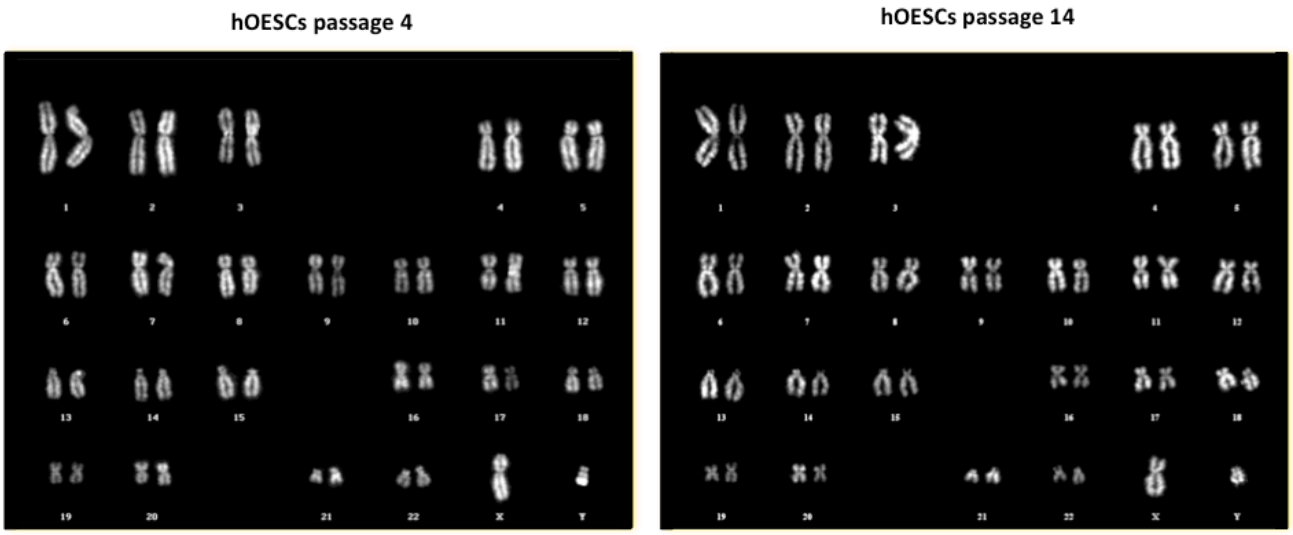

Figure 14: **Cell cycle and chromosomal stability.** (A) Cell cycle patterns were investigated by FACS after propidium iodide staining. Analyses were performed in hOESCs obtained from four different cases and the mean ± SEM was reported in the table. (B) Karyotype analyses.

4.2.4 hOESCs neural markers expression and immunophenotypic characterization

In addition, to improve hOESCs characterization, we also evaluated, by immunocytochemical methods, the expression of cellular markers, mostly neural markers (**Figure 15 A and B**). These markers include: GFAP (Glial fibrillary acidic protein), an intermediate filament protein, which is expressed by numerous cell type of the central nervous system; Nestin, an intermediate filament protein expressed in dividing cells during the early stages of development in the central nervous system (CNS), peripheral nervous system (PNS), and a marker for neural stem cells; and β-Tubulin III (Tuj1), a neuron specific Tubulin.

A

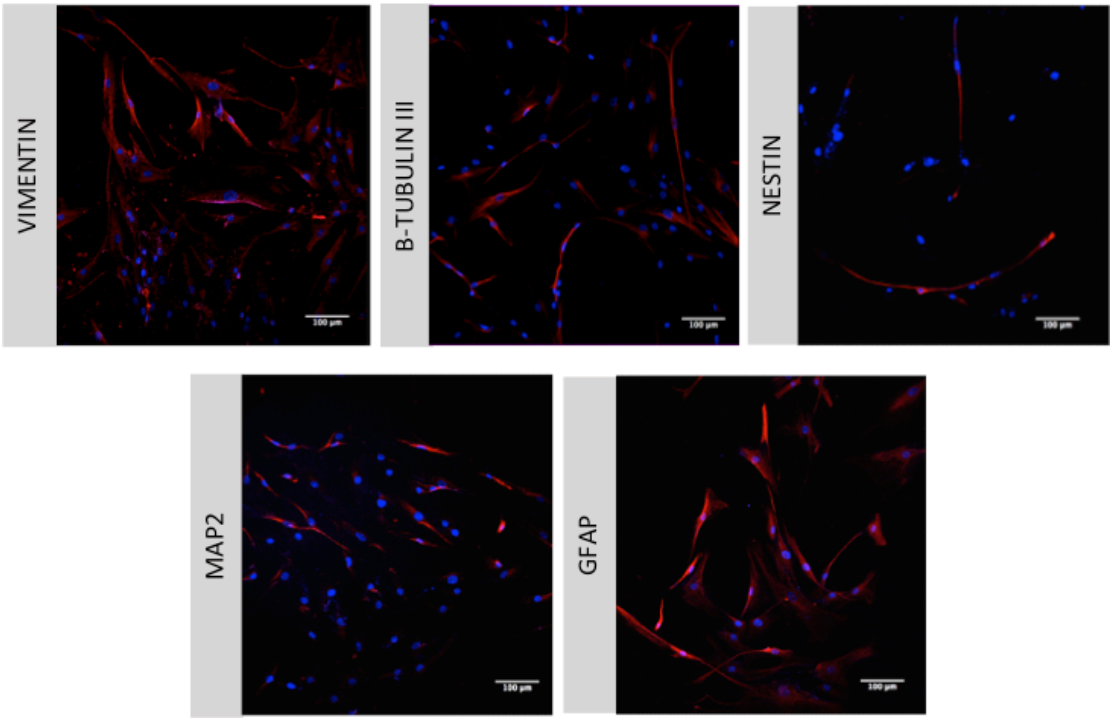

B

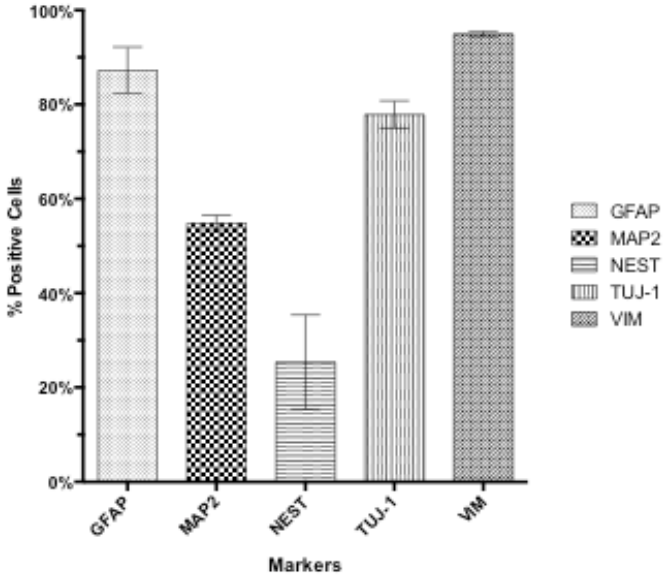

Vimentin	95.0 ± 0.6 %
Nestin	25.4 ± 10.0 %
GFAP	87.3 ± 4.9 %
MAP2	54.9 ± 1.7 %
βTubulin III	77.9 ± 2.9 %

Figure 15: hOESCs immunophenotypic characterization. *(A) hOESCs expression of neural markers. (A) The expression of neural (β-tubulin III, GFAP, MAP2), stem (nestin) and mesenchymal (vimentin) markers was investigated by immunofluorescence from the same case. (B) Quantification was performed by counting the number of cells positive for the staining. Positivity was expressed as a percent of the total cells. Data are expressed as the mean of three independent experiments for each case (n=9) with similar results ± SEM. Scale bars are 100 µm*

About 95% of cells expressed vimentin, a mesenchymal marker, as well as GFAP and TUJ1 that were highly expressed (around 87% and 78%, respectively). We observed a positive staining also for other neural markers, such as MAP2 (around 55%) and, even if with lower values, for nestin (25% circa) (**Figure 15 B**).

4.2.5 Flow cytofluorimetry detection of cell surface markers

To investigate the expression of cell surface markers, purified hOESCs were studied by means of FACS analyses from six different subjects, at high (passage 15) and low passages (passage 3), randomly chosen and grown TCM medium at 90% confluence. Unfortunately, as for hADSCs, there is not a specific marker capable of identifying this cells population.

As can be seen from the graph in Figure 16, hOESCs at low passages express high values of known mesenchymal markers (such as CD44, CD73, CD90, CD105 and CD166). As expected, some endothelial (CD31, CD34) and hematopoietic (CD45) markers were very few represented, while some others (CD56, CD144, CD146, CD133) are partially found. (**Figure 16***)*. Moreover, since hOESCs were obtained from different patients, these data highlight that the expression of surface markers molecules was very similar all samples. Notably, no statistically significant differences ($p>0.05$) were found in surface markers expression between low and high passages.

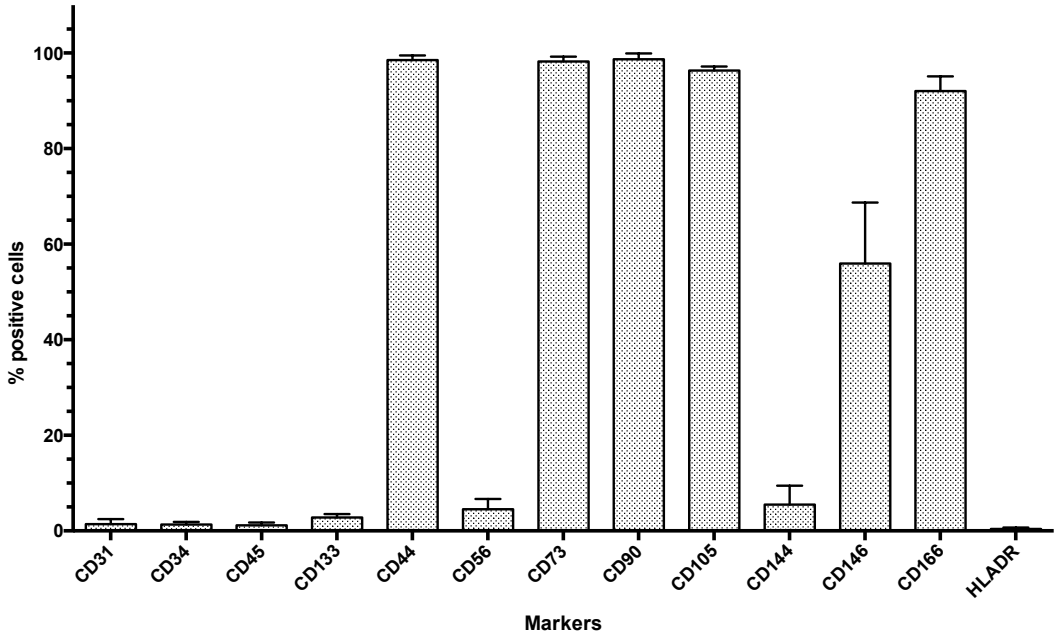

Figure 16: Cell surface phenotype of hOESCs. *Cell surface phenotype was investigated by FACS on hOESCs at early passages (passage 3). The assay was performed in six different cases, each case was investigated in triplicate.*

4.2.6 Pluripotency and stemness mRNA marker expression

To better understand hOESCs characteristics, we performed a mRNA expression analysis for some specific markers of pluripotency (such as SOX2, OCT4 and NANOG) and stemness (CD133).

By means of real-time RT-PCR (See Materials and Methods), we investigated some molecular determinants of self-renewal and stemness indicators. hOESCs expressed spontaneously embryonic stem cell genes, such as SOX2, NANOG and OCT4 (**Figure 17 A**). Moreover, they express in basal conditions also the mRNA of the stemness marker CD133 (**Figure 17 B**). The assay was performed in triplicate in five different cases with similar results. The quantitative expression of genes of interest relative to the housekeeping gene 18S was calculated.

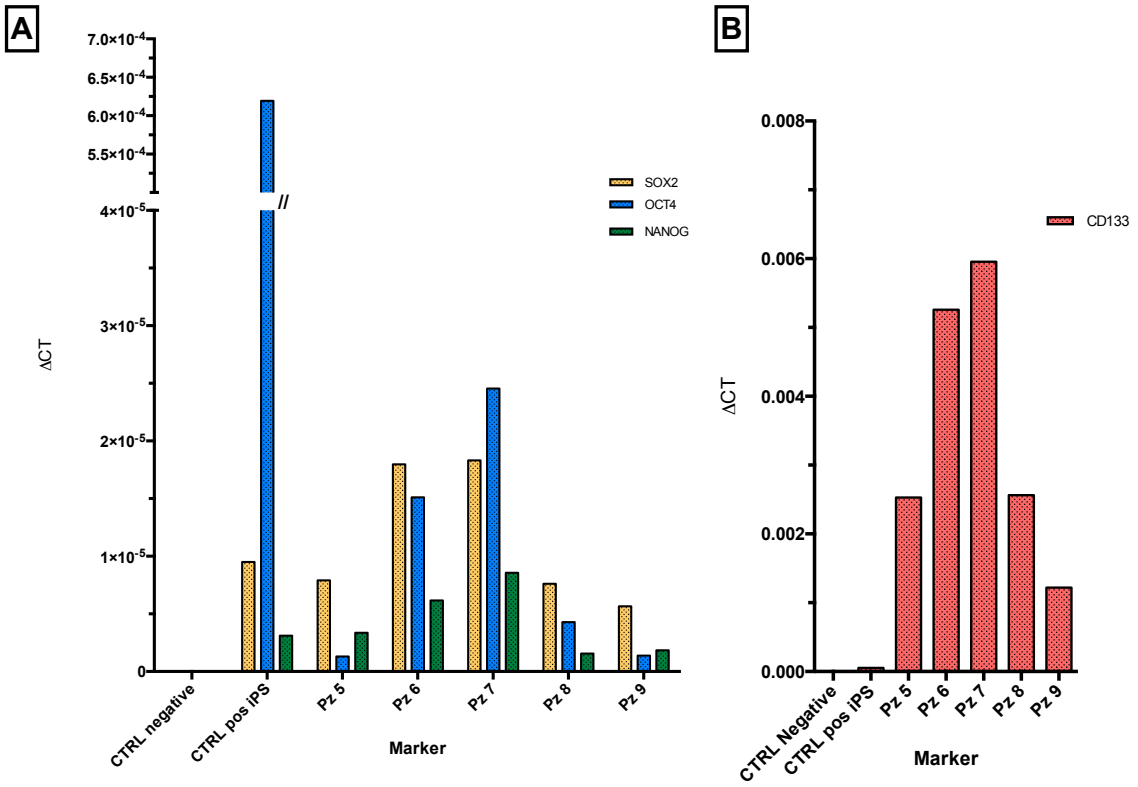

Figure 17: Pluripotency associated endogenous gene expression. *(A) Expression of SOX2, NANOG, OCT4 and (B) expression CD133 in hOESCs maintained in TCM was investigated by quantitative real-time RT-PCR. Data are expressed as the mean of four independent experiments ± SD.*

4.2.7 Spheroid formation and characterization

Bone marrow MSCs that are capable of forming spheroids in culture have been reported to have higher efficiency in differentiation [69]. Furthermore, mesenchymal stem cells show improved viability and developmental plasticity under defined serum-free media conditions after being grown as spheroid [91] while, in contrast, fibroblasts stop proliferation and undergo cell death when they are forced to form spheres [92]. Aiming at the generation of spheroids, hOESCs were incubated with serum-free medium normally used for the formation of neurospheres [66].

hOESCs at passage 2 spontaneously start to form spheres within 48 hours, with a diameter less than 50 μm (**Figure 18 A**). About 50% of cells formed large spheres after 7-10 days of culture, with a diameter

between 80-100 µm (**Figure 18 B**). The remaining cells formed small floating aggregates. The number of spheres was quantified.

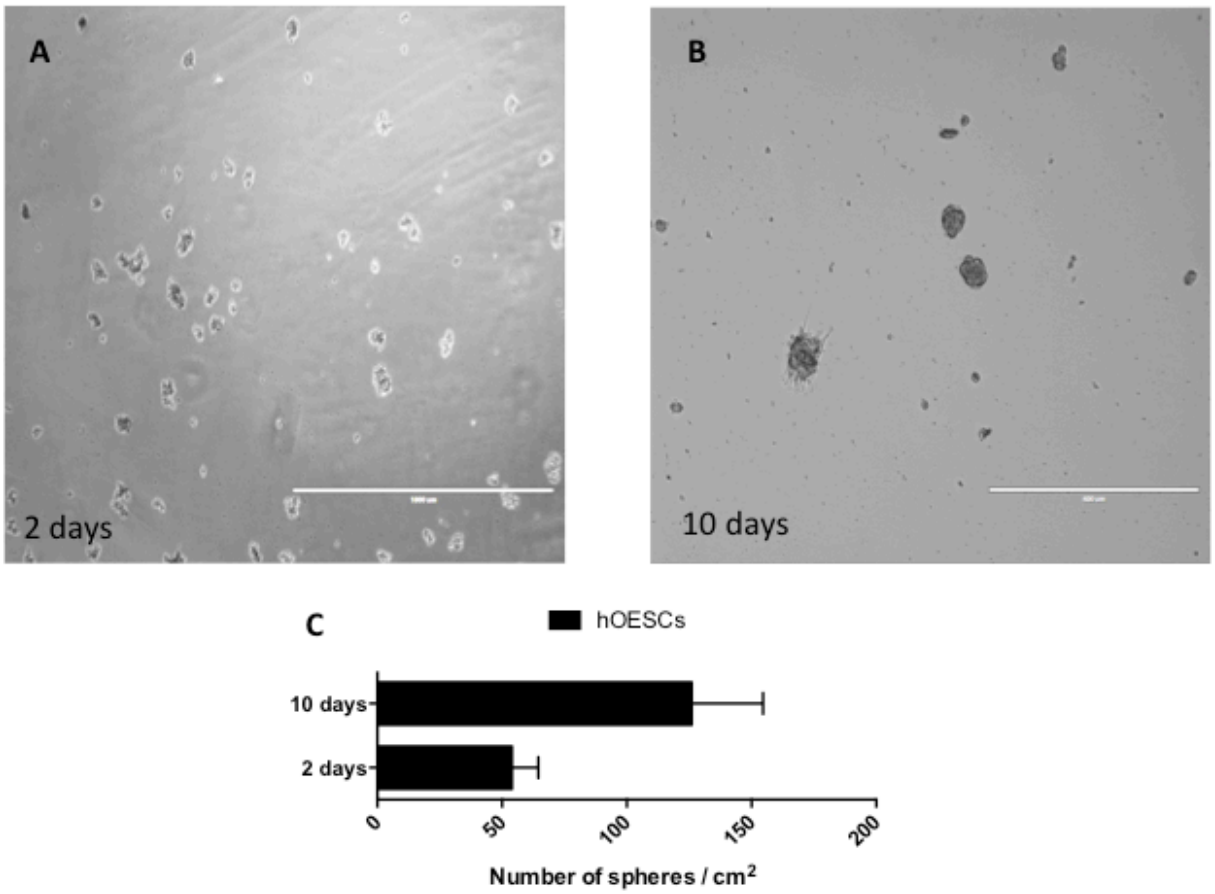

***Figure 18**: **Formation of hOESCs-derived spheroids (1st generation)**. (A) Spheroids formation at 48 hours. (B) Spheroids formation at 10 days. Bars are respectively 1000 µm and 400 µm. (C) The histogram reports the number of spheroids obtained in the different times of culture. Data are expressed as the mean of two independent experiments with similar results reporting mean ± SEM.*

Immunofluorescence detection of specific proteins such as nestin, vimentin, and GFAP showed that spheres are positive for these markers as expected. (**Figure 19**)

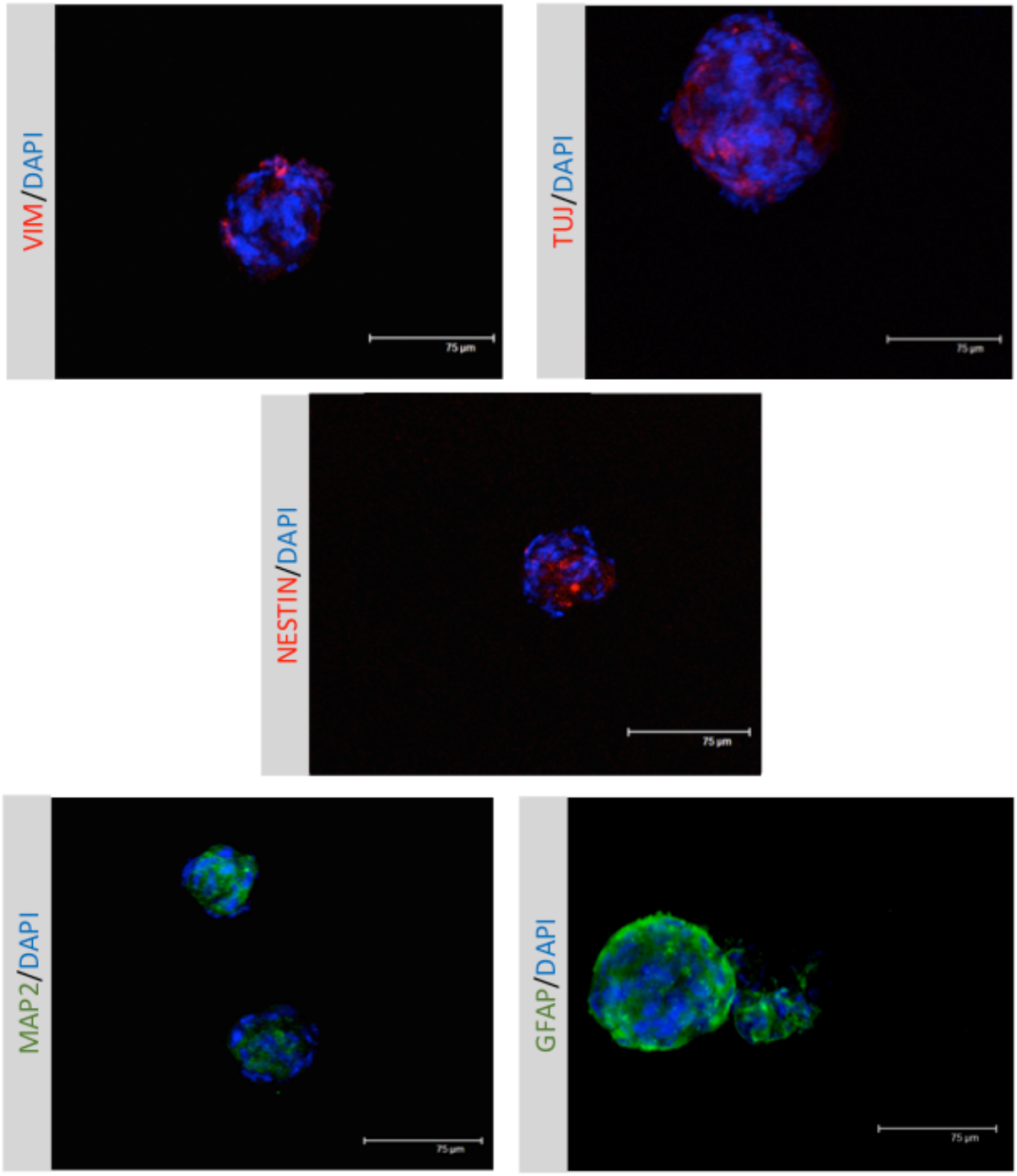

Figure 19: Immunofluorescence characterization of hOESCs-derived spheroids (1st generation). *The expression of nestin, vimentin, TUJ-1, Nestin, GFAP and MAP2 was investigated by immunofluorescence in spheres formed. Nestin, TUJ-1 and Vimentin are shown in red, MAP2 and GFAP are shown in green, and nuclei were stained with DAPI (blue). Scale bars: 25 µm.*

5 DISCUSSION

We have characterized two types of stem cells with the aim of studying their characteristics in terms of pluripotency features and to foresee their potential role as a cell therapy approach in regenerative medicine.

Adipose tissue-derived mesenchymal stem cells and the fat itself as a source of these cells, represent one of the major fields of research in regenerative medicine. A great advantage is represented by the minimal invasive and high accessibility to adipose tissue and its ready availability [108]. In the present study, we report that a population of stem cells, termed hADSCs, (with multilineage potential and expressing self-renewal transcription factors typical of multipotent stem cells), can be obtained from fresh or cryo-preserved human adipose tissue without enzymatic digestion. hADSCs have been investigated and characterized through different technical approaches, such as flow cytometry and immunocytochemistry. These hADSCs were isolated from the adipose tissue donated by several patients, and reproducibly fulfilled the general definition of MSCs by both phenotypic and differentiation capabilities criteria [109]. They also showed the expression of neural markers, as observed by confocal microscope analysis. Lipoaspirated adipose tissue showed a positivity to ß-tubulin III that was also maintained in lipoaspirate-derived hADSCs. The advantageous novelty of this method is that a population of stem cells retaining typical characteristics of surface markers of classical adipose tissue stem cells and MSCs can be obtained when adipose tissue is subjected to culture *in vitro*, either by processing through centrifugation or by direct plating, without enzymatic digestion with collagenase [48] [55]. Flow cytometry analyses showed that hADSCs expressed classical mesenchymal markers such as CD44, CD73, CD90, CD105 and CD166 [109] [110], while endothelial (CD31, CD34, CD144, CD146) and hematopoietic (CD45, CD133) markers were much less represented. A hallmark of MSCs is their multi-potency and ability to give rise to tissue of mesenchymal origins, such as

osteoblastic and adipogenic lineages, these features were present in hADSCs. In addition, the immunofluorescence staining indicated the expression of neural stem markers in hADSCs which consequently co-expressed nestin, β-tubulin III and glial GFAP. The above phenotypic profile was reported by other authors in mesenchymal stem cells obtained from different sources, such as amniotic fluid [111], nucleus polposus [74], bone marrow [112] and adipose tissue [113]. The ability of undifferentiated MSC to express immature and mature proteins typical of other tissues without any induction may support their plasticity to differentiate easily in many various tissues [73].

Olfactory Ensheathing stem cells, the superior turbinate and olfactory mucosa itself, they represent the second part of this characterization study, for their importance in promoting regeneration and reconstruction in regenerative medicine, retaining broadly potent differentiative capacity as stem cell progenitors [59]. Also in this case, a great advantage is represented by the high accessibility to olfactory mucosa, the minimal invasive technique required and its ready disposability [57] [58].

Most of the efforts of regenerative and translational medicine are addressed to biomedical approaches and clinical therapies that may involve the use of stem cells and cell therapies. One of the best studied applications of cell transplantation is with Spinal Cord Injury (SCI). The peculiar properties and the plasticity of hOESCs may allow them to transform themselves within different morphological and antigenic types. As a result of years of research on animal models of SCI, finally hOESCs came to human clinical trials applications and in 2006 the first pilot clinical study with transplantation of autologous hOESCs [99] were settled. Since that, several step forward were made in the knowledge of hOESCs trasplantation. In 2014, Tabakow et al. published a clinical study where a 38-year-old man with a traumatic transection of the thoracic spinal cord was transplanted with an autologous culture containing olfactory Ensheathing cells and olfactory nerve fibroblasts [104]; in this trial, no adverse effects were found at 19 months post-transplantation and the patient improved his neurological scores,

with an improved trunk stability, the partial recovery of the voluntary movements of the lower extremities, and an increase of the muscle mass in the left thigh, as well as partial recovery of superficial and deep sensation. This pattern of recovery suggested functional regeneration of both efferent and afferent long-distance nerve fibers, also confirmed by imaging and neurophysiological examinations. Notably, there was no general and neurological deterioration, progressive myelopathy, spine instability, neuropathic pain, tumors, infection or stenosis in all observational periods. The surgical intervention included spinal cord untethering, resection of the intraparenchymal scar tissue, injection into the spinal cord stumps and the rim of spared tissue of a mixture of bulbar Olfactory Ensheathing Cells/Olfactory Nerve Fibroblasts (OECs/ONFs), and reconnection of the stumps with four strips of sural nerves and was followed by a long and intense neurorehabilitation program. Each single intervention had its importance but, as the authors of this work state, could not be in itself sufficient if applied without the others. The transplanted cultures contained a mixture of OECs and ONFs, as ONFs form a surrounding cover on the outer surface of the OECs, with the nerve fibers on the inner surface. After transplantation into the corticospinal tract or optic nerve lesions, ONFs precede and establish a sort of channel for the advance of OECs [119] [120], and the two cells act together as essential and complementary components of a proregenerative tissue even if the mechanism of these complex interactions between OECs and ONFs is unknown. It certainly involves intimate surface-to-surface contact and paracrine mechanisms, depending on the interactions between membrane-bound molecules and leading to a basal lamina forming on the surface of the OECs facing the ONFs. The neurological recovery in the patient transplanted with OECs/ONFs indicates regeneration of central nervous system fibers that crossed the host/peripheral nerve interfaces and grew for a considerable distance to make functional connections in the cord [104].

For the reasons mentioned above, we set up a characherization of stem cells obtained from the superior turbinate tissue. In this study, we describe for the first time that a population of stem cells, termed

hOESCs, can be obtained and cultured from human posterosuperior septum or superior nasal concha and lamina propria biopsies and have been investigated and characterized through different technical approaches.

The method set up in this work allows the isolation of a stem cells population with high efficiency: as a matter of fact, it was possible to obtain $1\text{-}2\times10^4$ cells from each 3-4 mm^2 biopsy specimen after two weeks of culture at passage 0. Our isolation method differs from the other few protocols involving superior turbinate biopsies [115] [116] for using other digestive enzymes, in addition to the different anatomical site of the biopsy that, in most of the studies, are the inferior and middle turbinate. Moreover, our protocol avoids the use of coated flasks, which are used in the majority of works on hOESCs. Thus, we worked in the recommended direction of minimal manipulation of human cells tissues and cellular and tissue-based products [117] [118].

hOESCs isolated from the olfactory mucosa donated by nine patients, reproducibly show both the expression of neural and mesenchymal markers, as observed by confocal microscope with immunofluorescence staining for β-tubulin III, GFAP, MAP2, nestin and for vimentin. This population of stem cells retains typical characteristics of surface markers of classical mesenchymal stem cells: as seen by flow cytometry analyses, they express high values of known mesenchymal markers such as CD44, CD73, CD90, CD105 and CD166 [109] [110], other like some endothelial (CD31, CD34) and hematopoietic (CD45) markers were very few represented, while some others (CD56, CD144, CD146, CD133) are partially found. hOESCs also express pluripotency associated endogenous gene expression, as we found self-renewal and stemness transcription factors typical of multipotent stem cells such as SOX2, OCT4, NANOG and CD133. Moreover, they are capable of forming spheroids when cultured with serum-free neurospheres medium, that is a well-known stemness assay as long as all stem cells can form spheroids, and the formed spheroids highly express nestin, vimentin, TUJ-1, Nestin, GFAP and MAP2.

The ability of olfactory Ensheathing stem cells to express such a wide variety of proteins typical of other tissues and with different origin is in line with previusly reports describing that these cells are mesenchymal stem cells with ectodermal characteristics, neural crest-derived MSCs found in the branchial arch during development and named ectomesenchymal stem cells [84]. Interestingly, it has been shown by other groups that these ecto-mesenchymal stem cells have the capacity to differentiate both into ectoderm and mesoderm cell types [85].

Taken togheter, the features of the hADSCs and hOESCs studied in the present work suggest their pluripotency nature, making these cells a promising strategy in regenerative medicine applications. However, as our knowledge regarding the complex biology of adult stem cells increases, a deeper understanding of the underlying mechanisms of differentiation, immunomodulation (i.e. anti-inflammatory mechanisms) and engraftment *in vitro* and *in vivo* of these stem cells is essential for their future successful and safe application in different areas of medicine. Future studies will focus on these primary aspects and will investigate the effects and the *in vivo* capability of transplanted cells to survive, differentiate and migrate in animal models of neurodegenerative diseases.

6 REFERENCES

[1] W. A. Haseltine, Regenerative Medicine 2003: An Overview, e-biomed: The Journal of Regenerative Medicine 4 (3) (2003) 15–18. http://dx.doi.org/10.1089/152489003321222844

[2] H. L. Greenwood, H. Thorsteinsdottir, G. Perry, J. Renihan, P. A. Singer, A. S. Daar, Regenerative medicine: new opportunities for developing countries, International Journal of Biotechnology 8 (1/2) (2006) 60. http://dx.doi.org/10.1504/ijbt.2006.008964

[3] S. Petit-Zeman, Nat. Biotechnol. 19 (3) (2001) 201–206. http://dx.doi.org/10.1038/85619

[4] L. Alonso, E. Fuchs, Stem cells of the skin epithelium, Proceedings of the National Academy of Sciences 100 (Supplement 1) (2003) 11830–11835. http://dx.doi.org/10.1073/pnas.1734203100

[5] Harada S, Rodan GA. Control of osteoblast function and regulation of bone mass. Nature. 2003 May 15;423(6937):349-55. http://dx.doi.org/10.1038/nature01660

[6] F. Radtke, Self-Renewal and Cancer of the Gut: Two Sides of a Coin, Science 307 (5717) (2005) 1904–1909. http://dx.doi.org/10.1126/science.1104815

[7] D. L. Stocum, Tissue Restoration Through Regenerative Biology and Medicine, Springer Berlin Heidelberg, 2004. http://dx.doi.org/10.1007/978-3-642-18928-9

[8] I. Hyun, O. Lindvall, L. Ährlund-Richter, E. Cattaneo, M. Cavazzana-Calvo, G. Cossu, M. D. Luca, I. J. Fox, C. Gerstle, R. A. Goldstein, G. Hermerén, K. A. High, H. O. Kim, H. P. Lee, E. Levy-Lahad, L. Li, B. Lo, D. R. Marshak, A. McNab, M. Munsie, H. Nakauchi, M. Rao, H. M. Rooke, C. S. Valles, A. Srivastava, J. Sugarman, P. L. Taylor, A. Veiga, A. L. Wong, L. Zoloth, G. Q. Daley, New ISSCR Guidelines Underscore Major Principles for Responsible Translational Stem Cell Research, Cell Stem Cell 3 (6) (2008) 607–609. http://dx.doi.org/10.1016/j.stem.2008.11.009

[9] M. J. Evans, M. H. Kaufman, Establishment in culture of pluripotential cells from mouse embryos, Nature 292 (5819) (1981) 154–156. http://dx.doi.org/10.1038/292154a0

[10] G. R. Martin, Isolation of a pluripotent cell line from early mouse embryos cultured in medium conditioned by teratocarcinoma stem cells., Proceedings of the National Academy of Sciences 78 (12) (1981) 7634–7638. http://dx.doi.org/10.1073/pnas.78.12.7634

[11] M. S. Frankel, In Search of Stem Cell Policy, Science 287 (5457) (2000) 1397–1397.

http://dx.doi.org/10.1126/science.287.5457.1397

[12] M. F. Pittenger, Multilineage Potential of Adult Human Mesenchymal Stem Cells, Science 284 (5411) (1999) 143–147. http://dx.doi.org/10.1126/science.284.5411.143

[13] F. H. Gage, Mammalian Neural Stem Cells, Science 287 (5457) (2000) 1433–1438. http://dx.doi.org/10.1126/science.287.5457.1433

[14] C. Potten, H. Grant, The relationship between ionizing radiation-induced apoptosis and stem cells in the small and large intestine, Br J Cancer 78 (8) (1998) 993–1003. http://dx.doi.org/10.1038/bjc.1998.618

[15] M. Alison, C. Sarraf, Hepatic stem cells, Journal of Hepatology 29 (4) (1998) 676–682. http://dx.doi.org/10.1016/s0168-8278(98)80165-7

[16] J. Margolis, A. Spradling, Identification and behavior of epithelial stem cells in the Drosophila ovary., Development 121 (1995) 3797–807.

[17] S. Conrad, M. Renninger, J. Hennenlotter, T. Wiesner, L. Just, M. Bonin, W. Aicher, H. Bühring, U. Mattheus, A. Mack, H. Wagner, S. Minger, M. Matzkies, M. Reppel, J. Hescheler, K. Sievert, A. Stenzl, T. Skutella, Generation of pluripotent stem cells from adult human testis., Nature 456 (2008) 344–9.

[18] I. Weissman, Stem cells: units of development, units of regeneration, and units in evolution., Cell 100 (2000) 157–68.

[19] E. Fuchs, T. Tumbar, G. Guasch, Socializing with the neighbors: stem cells and their niche., Cell 116 (2004) 769–78.

[20] A. Hirao, F. Arai, T. Suda, Regulation of Cell Cycle in Hematopoietic Stem Cells by the Niche, Cell Cycle 3 (12) (2004) 1481–1483. http://dx.doi.org/10.4161/cc.3.12.1281

[21] S. J. Morrison, J. Kimble, Asymmetric and symmetric stem-cell divisions in development and cancer, Nature 441 (7097) (2006) 1068–1074. http://dx.doi.org/10.1038/nature04956

[22] B. Roelen, P. Dijke, Controlling mesenchymal stem cell differentiation by TGFBeta family members., J Orthop Sci 8 (2003) 740–8.

[23] I. Kratchmarova, Mechanism of Divergent Growth Factor Effects in Mesenchymal Stem Cell Differentiation, Science 308 (5727) (2005) 1472–1477. http://dx.doi.org/10.1126/science.1107627

[24] F. Mannello, G. Tonti, G. Bagnara, S. Papa, Role and function of matrix metalloproteinases in the differentiation and biological characterization of mesenchymal stem cells., Stem Cells 24 (2006) 475–81.

[25] C. A. Gregory, J. Ylostalo, D. J. Prockop, Adult Bone Marrow Stem/Progenitor Cells (MSCs) Are Preconditioned by Microenvironmental Niches in Culture: A Two-Stage Hypothesis for Regulation of MSC Fate, Science Signaling

2005 (294) (2005) pe37–pe37. http://dx.doi.org/10.1126/stke.2942005pe37

[26] A. Kortesidis, Stromal-derived factor-1 promotes the growth survival, and development of human bone marrow stromal stem cells, Blood 105 (10) (2005) 3793–3801. http://dx.doi.org/10.1182/blood-2004-11-4349

[27] Y. Jiang, Multipotent progenitor cells can be isolated from postnatal murine bone marrow muscle, and brain, Experimental Hematology 30 (8) (2002) 896–904. http://dx.doi.org/10.1016/s0301-472x(02)00869-x

[28] C. D. Keene, X. R. Ortiz-Gonzalez, Y. Jiang, D. A. Largaespada, C. M. Verfaillie, W. C. Low, Neural Differentiation and Incorporation of Bone Marrow-Derived Multipotent Adult Progenitor Cells After Single Cell Transplantation Into Blastocyst Stage Mouse Embryos, Cell Transplantation 12 (3) (2003) 201–213. http://dx.doi.org/10.3727/000000003108746768

[29] S. Wislet-Gendebien, G. Hans, P. Leprince, J.-M. Rigo, G. Moonen, B. Rogister, Plasticity of Cultured Mesenchymal Stem Cells: Switch from Nestin-Positive to Excitable Neuron-Like Phenotype, Stem Cells 23 (3) (2005) 392–402. http://dx.doi.org/10.1634/stemcells.2004-0149

[30] K. J. Cho, K. A. Trzaska, S. J. Greco, J. McArdle, F. S. Wang, J.-H. Ye, P. Rameshwar, Neurons Derived From Human Mesenchymal Stem Cells Show Synaptic Transmission and Can Be Induced to Produce the Neurotransmitter Substance P by Interleukin-1, Stem Cells 23 (3) (2005) 383–391. http://dx.doi.org/10.1634/stemcells.2004-0251

[31] Y. Sato, Human mesenchymal stem cells xenografted directly to rat liver are differentiated into human hepatocytes without fusion, Blood 106 (2) (2005) 756–763. http://dx.doi.org/10.1182/blood-2005-02-0572

[32] A. Friedenstein, R. Chailakhjan, K. Lalykina, The development of fibroblast colonies in monolayer cultures of guinea-pig bone marrow and spleen cells., Cell Tissue Kinet 3 (1970) 393–403.

[33] A. FRIEDENSTEIN, Osteogenic stem cells in the bone marrow, in: Bone and Mineral Research, Elsevier BV, 1990, pp. 243–272. http://dx.doi.org/10.1016/b978-0-444-81371-8.50012-1

[34] A. Friedenstein, R. Chailakhyan, N. Latsinik, A. Panasyuk, I. Keiliss-Borok, Stromal cells responsible for transferring the microenvironment of the hemopoietic tissues. Cloning in vitro and retransplantation in vivo., Transplantation 17 (1974) 331–40.

[35] A. J. Friedenstein, R. K. Chailakhjan, K. S. Lalykina, THE DEVELOPMENT OF FIBROBLAST COLONIES IN MONOLAYER CULTURES OF GUINEA-PIG BONE MARROW AND SPLEEN CELLS, Cell Proliferation 3 (4) (1970) 393–403. http://dx.doi.org/10.1111/j.1365-2184.1970.tb00347.x

[36] H. Castro-Malaspina, R. Gay, G. Resnick, N. Kapoor, P. Meyers, D. Chiarieri, S. McKenzie, H. Broxmeyer, M. Moore, Characterization of human bone marrow fibroblast colony-forming cells (CFU-F) and their progeny., Blood

56 (1980) 289–301.

[37] A. Caplan, Mesenchymal stem cells., J Orthop Res 9 (1991) 641–50.

[38] A. Batsali, M. Kastrinaki, H. Papadaki, C. Pontikoglou, Mesenchymal stem cells derived from Wharton's Jelly of the umbilical cord: biological properties and emerging clinical applications., Curr Stem Cell Res Ther 8 (2013) 144–55.

[39] K. Johe, T. Hazel, T. Muller, M. Dugich-Djordjevic, R. McKay, Single factors direct the differentiation of stem cells from the fetal and adult central nervous system., Genes Dev 10 (1996) 3129–40.

[40] B. Johnstone, T. M. Hering, A. I. Caplan, V. M. Goldberg, J. U. Yoo, In VitroChondrogenesis of Bone Marrow-Derived Mesenchymal Progenitor Cells, Experimental Cell Research 238 (1) (1998) 265–272. http://dx.doi.org/10.1006/excr.1997.3858

[41] M. Dominici, K. L. Blanc, I. Mueller, I. Slaper-Cortenbach, F. Marini, D. Krause, R. Deans, A. Keating, D. Prockop, E. Horwitz, Minimal criteria for defining multipotent mesenchymal stromal cells. The International Society for Cellular Therapy position statement, Cytotherapy 8 (4) (2006) 315–317. doi:10.1080/14653240600855905. http://dx.doi.org/10.1080/14653240600855905

[42] N. G. Singer, A. I. Caplan, Mesenchymal Stem Cells: Mechanisms of Inflammation, Annu. Rev. Pathol. Mech. Dis. 6 (1) (2011) 457–478. doi:10.1146/annurev-pathol-011110-130230.
http://dx.doi.org/10.1146/annurev-pathol-011110-130230

[43] P. A. Zuk, M. Zhu, H. Mizuno, J. Huang, J. W. Futrell, A. J. Katz, P. Benhaim, H. P. Lorenz, M. H. Hedrick, Multilineage Cells from Human Adipose Tissue: Implications for Cell-Based Therapies, Tissue Engineering 7 (2) (2001) 211–228. doi:10.1089/107632701300062859. http://dx.doi.org/10.1089/107632701300062859

[44] R. A. Musina, E. S. Bekchanova, G. T. Sukhikh, Comparison of Mesenchymal Stem Cells Obtained from Different Human Tissues, Bulletin of Experimental Biology and Medicine 139 (4) (2005) 504–509. doi:10.1007/s10517-005-0331-1. http://dx.doi.org/10.1007/s10517-005-0331-1

[45] A. C. Boquest, A. Shahdadfar, J. E. Brinchmann, P. Collas, Isolation of Stromal Stem Cells From Human Adipose Tissue, in: Nuclear Reprogramming, Springer Science Business Media, 2005, pp. 35–46. doi:10.1385/1-59745-005-7:35. http://dx.doi.org/10.1385/1-59745-005-7:35

[46] B. Strem, K. Hicok, M. Zhu, I. Wulur, Z. Alfonso, R. Schreiber, J. Fraser, M. Hedrick, Multipotential differentiation of adipose tissue-derived stem cells., Keio J Med 54 (2005) 132–41.

[47] A. Sterodimas, F. J. de, B. Nicaretta, I. Pitanguy, Tissue engineering with adipose-derived stem cells (ADSCs): current and future applications., J Plast Reconstr Aesthet Surg 63 (2010) 1886–92.

[48] P. Zuk, M. Zhu, H. Mizuno, J. Huang, J. Futrell, A. Katz, P. Benhaim, H. Lorenz, M. Hedrick, Multilineage cells from human adipose tissue: implications for cell-based therapies., Tissue Eng 7 (2001) 211–28.

[49] D. De Ugarte, K. Morizono, A. Elbarbary, Z. Alfonso, P. Zuk, M. Zhu, J. Dragoo, P. Ashjian, B. Thomas, P. Benhaim, I. Chen, J. Fraser, M. Hedrick, Comparison of multi-lineage cells from human adipose tissue and bone marrow., Cells Tissues Organs 174 (2003) 101–9.

[50] R. Izadpanah, C. Trygg, B. Patel, C. Kriedt, J. Dufour, J. M. Gimble, B. A. Bunnell, Biologic properties of mesenchymal stem cells derived from bone marrow and adipose tissue, Journal of Cellular Biochemistry 99 (5) (2006) 1285–1297. http://dx.doi.org/10.1002/jcb.20904

[51] J. B. Mitchell, K. McIntosh, S. Zvonic, S. Garrett, Z. E. Floyd, A. Kloster, Y. D. Halvorsen, R. W. Storms, B. Goh, G. Kilroy, X. Wu, J. M. Gimble, Immunophenotype of Human Adipose-Derived Cells: Temporal Changes in Stromal-Associated and Stem Cell-Associated Markers, Stem Cells 24 (2) (2006) 376–385. http://dx.doi.org/10.1634/stemcells.2005-0234

[52] H. Mizuno, Adipose-derived stem and stromal cells for cell-based therapy: current status of preclinical studies and clinical trials., Curr Opin Mol Ther 12 (2010) 442–9.

[53] H. Mizuno, M. Tobita, A. C. Uysal, Concise Review: Adipose-Derived Stem Cells as a Novel Tool for Future Regenerative Medicine, STEM CELLS 30 (5) (2012) 804–810. http://dx.doi.org/10.1002/stem.1076

[54] P. A. Zuk, The Adipose-derived Stem Cell: Looking Back and Looking Ahead, Molecular Biology of the Cell 21 (11) (2010) 1783–1787. http://dx.doi.org/10.1091/mbc.e09-07-0589

[55] P. A. Zuk, Human Adipose Tissue Is a Source of Multipotent Stem Cells, Molecular Biology of the Cell 13 (12) (2002) 4279–4295. http://dx.doi.org/10.1091/mbc.e02-02-0105

[56] K. Safford, H. Rice, Stem Cell Therapy for Neurologic Disorders: Therapeutic Potential of Adipose-Derived Stem Cells, Current Drug Targets 6 (1) (2005) 57–62. http://dx.doi.org/10.2174/1389450053345028

[57] N. E. Rawson, G. Gomez, Cell and molecular biology of human olfaction, Microscopy Research and Technique 58 (3) (2002) 142. http://dx.doi.org/10.1002/jemt.10132

[58] G. Raisman, Olfactory ensheathing cells — another miracle cure for spinal cord injury?, Nature Reviews Neuroscience 2 (5) (2001) 369–375. http://dx.doi.org/10.1038/35072576

[59] J. E. Schwob, W. Jang, Stem Cells of the Adult Olfactory Epithelium, in: Neural Development and Stem Cells, Springer Science Business Media, 2006, pp. 219–233. http://dx.doi.org/10.1385/1-59259-914-1:219

[60] A. Ramón-Cueto, J. Avila, Olfactory ensheathing glia: properties and function, Brain Research Bulletin 46 (3)

(1998) 175–187. http://dx.doi.org/10.1016/s0361-9230(97)00463-2

[61] L. A. Carter, Olfactory Horizontal Basal Cells Demonstrate a Conserved Multipotent Progenitor Phenotype, Journal of Neuroscience 24 (25) (2004) 5670–5683. http://dx.doi.org/10.1523/jneurosci.0330-04.2004

[62] C. T. Leung, P. A. Coulombe, R. R. Reed, Contribution of olfactory neural stem cells to tissue maintenance and regeneration, Nature Neuroscience 10 (6) (2007) 720–726. http://dx.doi.org/10.1038/nn1882

[63] Z. Su, C. He, Olfactory ensheathing cells: Biology in neural development and regeneration, Progress in Neurobiology 92 (4) (2010) 517–532. http://dx.doi.org/10.1016/j.pneurobio.2010.08.008

[64] Y. Li, T. Carlstedt, C.-H. Berthold, G. Raisman, Interaction of transplanted olfactory-ensheathing cells and host astrocytic processes provides a bridge for axons to regenerate across the dorsal root entry zone, Experimental Neurology 188 (2) (2004) 300–308. http://dx.doi.org/10.1016/j.expneurol.2004.04.021

[65] Navone SE, Marfia G, Nava S, Invernici G, Cristini S, Balbi S, Sangiorgi S, Ciusani E, Bosutti A, Alessandri G, Slevin M, Parati EA. Human and mouse brain-derived endothelial cells require high levels of growth factors medium for their isolation, in vitro maintenance and survival. Vasc Cell. 2013; 5(1):10. doi: 10.1186/2045-824X-5-10.

[66] S. Carelli, F. Messaggio, A. Canazza, D. Hebda, F. Caremoli, E. Latorre, M. Grimoldi, M. Colli, G. Bulfamante, C. Tremolada, G. A. Di, A. Gorio, Characteristics and Properties of Mesenchymal Stem Cells Derived From Microfragmented Adipose Tissue., Cell Transplant 24 (2015) 1233–52.

[67] A. Canazza, G. Bedini, F. Caremoli, S. Nava, E. Latorre, V. Tosetti, M. Taiana, M. Dossena, A. Bersano, D. Pareyson, M.G. Grimoldi, F. Corsi, A.M. Di Giulio, E.A. Parati, S. Carelli, A. Gorio. A novel efficient method to isolate human adipose-derived stromal cells from periumbilical biopsies without enzymatic digestion. CellR4 2015; 3 (1): e1397

[68] X. F. Yang, X. He, J. He, L. H. Zhang, X. J. Su, Z.Y. Dong, Y.J. Xu, Y. Li, Y.L. Li. High efficient isolation and systematic identification of human adipose-derived mesenchymal stem cells. J. Biomed. Sci. 2011, 18:59.

[69] Oswald, J.; Boxberger, S.; Jørgensen, B.; Feldmann, S.; Ehninger, G.; Bornhäuser, M.; Werner, C. Mesenchymal stem cells can be differentiated into endothelial cells in vitro. Stem Cells. 22:377-384; 2004

[70] Katz, A. J.; Tholpady, A.; Tholpady, S. S.; Shang, H.; Ogle, R. C. Cell surface and transcriptional characterization of human adipose-derived adherent stromal (hADAS) cells. Stem Cells. 23:412–423; 2005.

[71] Kawaji, A.; Ohnaka, Y.; Osada, S.; Nishizuka, M.; Imagawa, M. Gelsolin, an actin regulatory protein, is required for differentiation of mouse 3T3-L1 cells into adipocytes. Biol. Pharm. Bull. 33:773-779; 2010.

[72] Kim, C. Y.; Le, T. T.; Chen, C.; Cheng, J. X.; Kim, K. H. Curcumin inhibits adipocyte differentiation through

modulation of mitotic clonal expansion. J. Nutr. Biochem. 22:910-20; 2011.

[73] Jiang, Y, Jahagirdar, B. N.; Reinhardt, R. L.; Schwartz, R. E.; Keene, C. D.; Ortiz-Gonzalez, X. R.; Reyes, M.; Lenvik, T.; Lund, T.; Blackstad, M.; Du, J.; Aldrich, S.; Lisberg, A.; Low, W. C.; Largaespada D. A.; Verfaillie C. M. Pluripotency of mesenchymal stem cells derived from adult marrow. Nature. 418:41-49; 2002.

[74] Navone, S. E.; Marfia, G.; Canzi, L.; Ciusani, E.; Canazza, A.; Visintini, S.; Campanella, R.; Parati, E. A. Expression of neural and neurotrophic markers in nucleus pulposus cells isolated from degenerated intervertebral disc. J. Orthop. Res. 30:1470-1477; 2012.

[75] Bianco J.I., Perry C., Harkin D.G., Mackay-Sim A., Feron F. Neurotrophin 3 promotes purification and proliferation of olfactory Ensheathing cells from human nose. Glia 2004. 45:111-123.

[76] Vincent AJ, West AK, Chuah MI. Morphological and functional plasticity of olfactory ensheathing cells. J Neurocytol. 2005 Mar;34(1-2):65-80

[77] Au E, Roskams AJ. Olfactory ensheathing cells of the lamina propria in vivo and in vitro. Glia. 2003 Feb;41(3):224-36

[78] van den Pol AN, Santarelli JG. Olfactory ensheathing cells: time lapse imaging of cellular interactions, axonal support, rapid morphologic shifts, and mitosis. J Comp Neurol. 2003 Mar 31;458(2):175-94.

[79] Hauser S, Widera D, Qunneis F, Müller J, Zander C, Greiner J, Strauss C, Lüningschrör P, Heimann P, Schwarze H, Ebmeyer J, Sudhoff H, Araúzo-Bravo MJ, Greber B, Zaehres H, Schöler H, Kaltschmidt C, Kaltschmidt B. Isolation of novel multipotent neural crest-derived stem cells from adult human inferior turbinate. Stem Cells Dev. 2012 Mar 20;21(5):742-56. doi: 10.1089/scd.2011.0419

[80] Murrell W, F F.ron, A Wetzig, N Cameron, K Splatt, B Bellette, J Bianco, C Perry, G Lee and A Mackay-Sim. (2005). Multipotent stem cells from adult olfactory mucosa. Dev Dyn 233:496–515

[81] Cuschieri A and LH Bannister. (1975). The development of the olfactory mucosa in the mouse: electron microscopy. J Anat 119(Pt 3):471–498.

[82] Cuschieri A and LH Bannister. (1975). The development of the olfactory mucosa in the mouse: light microscopy. J Anat 119 (Pt 2):277–286.

[83] Whitlock KE. (2004). A new model for olfactory placode development. Brain Behav Evol 64:126–140.

[84] Le Douarin NM, GW Calloni and E Dupin. (2008). The stem cells of the neural crest. Cell Cycle 7:1013–1019.

[85] Calloni GW, NM Le Douarin and E Dupin. (2009). High frequency of cephalic neural crest cells shows coexistence of neurogenic, melanogenic, and osteogenic differentiation capacities. Proc Natl Acad Sci USA 106:8947–8952.

[86] Franssen EH. de Bree FM. Verhaagen J. Olfactory ensheathing glia: their contribution to primary olfactory nervous system regeneration and their regenerative potential following transplantation into the injured spinal cord. Brain Res Rev. 2007;56:236–258.

[87] Kocsis JD. Lankford KL. Sasaki M, et al. Unique in vivo properties of olfactory ensheathing cells that may contribute to neural repair and protection following spinal cord injury. Neurosci Lett. 2009;456:137–142.

[88] Lindsay SL. Riddell JS. Barnett SC. Olfactory mucosa for transplant-mediated repair: a complex tissue for a complex injury? Glia. 2010;58:125–134.

[89] Barraud P. Seferiadis AA. Tyson LD, et al. Neural crest origin of olfactory ensheathing glia. Proc Natl Acad Sci U S A. 2011;107:21040–21045.

[90] Delorme B. Nivet E. Gaillard J, et al. The human nose harbors a niche of olfactory ectomesenchymal stem cells displaying neurogenic and osteogenic properties. Stem Cells Dev. 2010;19:853–866.

[91] Wang W, Itaka K, Ohba S, Nishiyama N, Chung UI, Yamasaki Y, Kataoka K. 3D spheroid culture system on micropatterned substrates for improved differentiation efficiency of multipotent mesenchymal stem cells. Biomaterials. 2009;30(14):2705-15. doi: 10.1016/j.biomaterials.2009.01.030.

[92] Kapur SK, Wang X, Shang H, Yun S, Li X, Feng G, Khurgel M, Katz AJ. Human adipose stem cells maintain proliferative, synthetic and multipotential properties when suspension cultured as self-assembling spheroids. Biofabrication. 2012;4(2):025004. doi: 10.1088/1758-5082/4/2/025004

[93] Takahashi K, Tanabe K, Ohnuki M, Narita M, Ichisaka T, Tomoda K, Yamanaka S. (2007). Induction of Pluripotent Stem Cells from Adult Human Fibroblasts by Defined Factors. Cell. 131:861–872.

[94] Li J, Lepski G. Cell transplantation for spinal cord injury: a systematic review. Biomed Res Int. 2013;2013:786475. doi: 10.1155/2013/786475

[95] National Spinal Cord Injury Statistic Centre: Spinal Cord Injury Facts and Figures at a Glance, https://www.nscisc.uab.edu/PublicDocuments/nscisc_home/pdf/Facts%202011%20Feb%20Final.pdf, 2012.

[96] Su Z, He C. Olfactory ensheathing cells: biology in neural development and regeneration. Prog Neurobiol. 2010;92(4):517-32. doi: 10.1016/j.pneurobio.2010.08.008.

[97] Liu J, Chen P, Wang Q, Chen Y, Yu H, Ma J, Guo M, Piao M, Ren W, Xiang L. Meta analysis of olfactory ensheathing cell transplantation promoting functional recovery of motor nerves in rats with complete spinal cord transection. Neural Regen Res. 2014 Oct 15;9(20):1850-8. doi: 10.4103/1673-5374.143434.

[98] Richter MW, Fletcher PA, Liu J, Tetzlaff W, Roskams AJ. Lamina propria and olfactory bulb ensheathing cells

exhibit differential integration and migration and promote differential axon sprouting in the lesioned spinal cord. J Neurosci. 2005 Nov 16;25(46):10700-11

[99] Lima C, Pratas-Vital J, Escada P, Hasse-Ferreira A, Capucho C, Peduzzi JD. Olfactory Mucosa Autografts in Human Spinal Cord Injury: A Pilot Clinical Study. *The Journal of Spinal Cord Medicine*. 2006;29(3):191-203.

[100] Conley, B.J., Young, J.C., Trounson, A.O., Mollard, R., 2004. Derivation, propagation and differentiation of human embryonic stem cells. Int. J. Biochem. Cell Biol. 36, 555–567.

[101] Tabar V, Studer L. Pluripotent stem cells in regenerative medicine: challenges and recent progress. Nat Rev Genet. 2014 Feb;15(2):82-92. doi: 10.1038/nrg3563

[102] Tabakow P, Jarmundowicz W, Czapiga B, Fortuna W, Miedzybrodzki R, Czyz M, Huber J, Szarek D, Okurowski S, Szewczyk P, Gorski A, Raisman G. Transplantation of autologous olfactory ensheathing cells in complete human spinal cord injury. Cell Transplant. 2013;22(9):1591-612. doi: 10.3727/096368912X663532

[103] Rao Y, Zhu W, Liu H, Jia C, Zhao Q, Wang Y. Clinical application of olfactory ensheathing cells in the treatment of spinal cord injury. J Int Med Res. 2013 Apr;41(2):473-81. doi: 10.1177/0300060513476426.

[104] Tabakow P, Raisman G, Fortuna W, Czyz M, Huber J, Li D, Szewczyk P, Okurowski S, Miedzybrodzki R, Czapiga B, Salomon B, Halon A, Li Y, Lipiec J, Kulczyk A, Jarmundowicz W. Functional regeneration of supraspinal connections in a patient with transected spinal cord following transplantation of bulbar olfactory ensheathing cells with peripheral nerve bridging. Cell Transplant. 2014;23(12):1631-55. doi: 10.3727/096368914X685131

[105] Wang M, Lu C, Roisen F. Adult human olfactory epithelial-derived progenitors: a potential autologous source for cell-based treatment for Parkinson's disease. Stem Cells Transl Med. 2012 Jun;1(6):492-502. doi: 10.5966/sctm.2012-0012.

[106] Murrell W, Wetzig A, Donnellan M, Féron F, Burne T, Meedeniya A, Kesby J, Bianco J, Perry C, Silburn P, Mackay-Sim A. Olfactory mucosa is a potential source for autologous stem cell therapy for Parkinson's disease. Stem Cells. 2008 Aug;26(8):2183-92. doi: 10.1634/stemcells.2008-0074.

[107] Nivet E, Vignes M, Girard SD, Pierrisnard C, Baril N, Devèze A, Magnan J, Lanté F, Khrestchatisky M, Féron F, Roman FS. Engraftment of human nasal olfactory stem cells restores neuroplasticity in mice with hippocampal lesions. J Clin Invest. 2011 Jul;121(7):2808-20. doi: 10.1172/JCI44489.

[108] Safford KM, Rice HE. Stem cell therapy for neurologic disorders: therapeutic potential of adipose-derived stem cells. Curr Drug Targets. 2005 Feb;6(1):57-62

[109] Bianco P, Robey PG, Simmons PJ. Mesenchymal stem cells: revisiting history, concepts, and assays. Cell Stem Cell.

2008 Apr 10;2(4):313-9. doi: 10.1016/j.stem.2008.03.002

[110] Maurer MH. Proteomic definitions of mesenchymal stem cells. Stem Cells Int. 2011 Mar 3;2011:704256. doi: 10.4061/2011/704256

[111] Bottai D, Cigognini D, Nicora E, Moro M, Grimoldi MG, Adami R, Abrignani S, Marconi AM, Di Giulio AM, Gorio A. Third trimester amniotic fluid cells with the capacity to develop neural phenotypes and with heterogeneity among sub-populations. Restor Neurol Neurosci. 2012;30(1):55-68. doi: 10.3233/RNN-2011-0620.

[112] Tondreau T, Lagneaux L, Dejeneffe M, Massy M, Mortier C, Delforge A, Bron D. Bone marrow-derived mesenchymal stem cells already express specific neural proteins before any differentiation. Differentiation. 2004 Sep;72(7):319-26

[113] Jiang J, Lv Z, Gu Y, Li J, Xu L, Xu W, Lu J, Xu J. Adult rat mesenchymal stem cells differentiate into neuronal-like phenotype and express a variety of neuro-regulatory molecules in vitro. Neurosci Res. 2010 Jan;66(1):46-52. doi: 10.1016/j.neures.2009.09.1711

[114] Alessandri G, Pagano S, Bez A, Benetti A, Pozzi S, Iannolo G, Baronio M, Invernici G, Caruso A, Muneretto C, Bisleri G, Parati E. Isolation and culture of human muscle-derived stem cells able to differentiate into myogenic and neurogenic cell lineages. Lancet. 2004 Nov 20-26;364(9448):1872-83

[115] Pinna Fde R, Ctenas B, Weber R, Saldiva PH, Voegels RL. Olfactory neuroepithelium in the superior and middle turbinates: which is the optimal biopsy site? Int Arch Otorhinolaryngol. 2013 Apr;17(2):131-8. doi: 10.7162/S1809-97772013000200004

[116] Lane AP, Gomez G, Dankulich T, Wang H, Bolger WE, Rawson NE. The superior turbinate as a source of functional human olfactory receptor neurons. Laryngoscope. 2002 Jul;112(7 Pt 1):1183-9.

[117] Minimal Manipulation of Human Cells, Tissues, and Cellular and Tissue-Based Products: Draft Guidance - http://www.fda.gov/BiologicsBloodVaccines/GuidanceComplianceRegulatoryInformation/Guidances/CellularandGeneTherapy/ucm427692.htm

[118] Advanced therapy medicinal products (ATMP) legislation - http://eur-lex.europa.eu/LexUriServ/LexUriServ.do?uri=OJ:L:2007:324:0121:0137:en:PDF

[119] Li Y, Field PM, Raisman G. Regeneration of adult rat corticospinal axons induced by transplanted olfactory ensheathing cells. J Neurosci. 1998 Dec 15;18(24):10514-24.

[120] Li Y, Sauvé Y, Li D, Lund RD, Raisman G. Transplanted olfactory ensheathing cells promote regeneration of cut adult rat optic nerve axons. J Neurosci. 2003 Aug 27;23(21):7783-8.

7 PUBLICATIONS

Papers:

- **Caremoli F.**, Bassoli A, Borgonovo G., Morini G., Torri L. *Do you like it bitter? A preliminary study on food preferences for bitter taste in a young population*. Hórisma Book series "World food trends and the future of food", 2015. (article accepted).

- Carelli S.*, **Caremoli F.***, Latorre E.*, Giallongo T., Colli M., Canazza A., Provenzani A., Di Giulio A.M., and Gorio A. "*Human antigen R binding and regulation of SOX2 mRNA in human mesenchymal stem cells*". Under revision by Molecular Pharmacology, 2015. *equal contribution.

- Latorre E., Carelli S., Giallongo T., **Caremoli F.**, Provenzani A., Di Giulio A.M. and Gorio A. *Long-non-coding RNAs and HuR interaction may regulate neural stem cell differentiation*. Submitted to Journal of Stem Cells Research and Therapy 2015.

- Canazza A.*, Bedini G.*, **Caremoli F.**, Nava S., Latorre E., Tosetti V., Taiana M., Dossena M., Bersano A., Pareyson D., Grimoldi M.G., Corsi F., Di Giulio A.M., Parati E.A., Carelli S., Gorio A. *A novel efficient method to isolate human adipose-derived stromal cells from periumbilical biopsies without enzymatic digestion*. CellR4 2015; 3 (1): e1397. *equal contribution

- Carelli S., Giallongo T., Latorre E., **Caremoli F.**, Gerace C., Basso M.D., Di Giulio A.M. and Gorio A. *Adult Mouse Post Mortem Neural Precursors Survive, Differentiate, Counteract Cytokine Production and Promote Functional Recovery after Transplantation in Experimental Traumatic Spinal Cord Injury*. J Stem Cell Res Transplant. 2014;1(2): 1008.

- Carelli S., Messaggio F., Canazza A., Hebda D.M., **Caremoli F.**, Latorre E., Grimoldi M.G., Colli M., Bulfamante G., Tremolada C., Di Giulio A.M. and Gorio A. *Characteristics and Properties of Mesenchymal Stem Cells Derived from Micro-fragmented Adipose Tissue.* Cell Transplantation, 2014, Epub ahead of print, PubMed PMID: 24806078

- Bassoli A., Borgonovo G., **Caremoli F.**, Mancuso G. *The taste of D- and L- amino acids: in vitro binding assays with cloned human bitter (TAS2Rs) and sweet (TAS1R2/TAS1R3) receptors*. Food Chem., 2014 May 1;150:27-33. doi:10.1016/j.foodchem.2013.10.106.

Posters:

- **Caremoli F.,** Saibene A.M, Carelli S., Nava S., Felisati G., Di Giulio A.M. and Gorio A. *Purification, characterization and culture of ensheathing cells from human olfactory mucosa biopsies.* 1° congresso Dipartimento di Scienze della Salute DISS, November 13th, 2015.

- **Caremoli F.***, De Angelis A.*, Latorre E., Giallongo T., Di Giulio A.M., Carelli S., Gorio A.. *Human adipose-derived stem cells obtained without enzymatic digestion present high multipotent features*. Forum of Italian Researchers on Mesenchymal and Stromal Stem Cells, 6th Meeting FIRST - Milano, May 12th – 13th, 2014 *equal contibution

- Carelli S., Giallongo T., Viaggi C., Gerace C., Hebda D.M., **Caremoli F.**, Corsini G.U., Di Giulio A.M. and Gorio A. *Exogenous Adult Mouse Post Mortem Neural promote functional recovery in a mouse model of Parkinson disease and differentiate in TH-positive neurons*. Forum of Neuroscience, 9th FENS, Milan July 5-9, 2014

- Carelli S., **Caremoli F.**, De Angelis A., Latorre E., Gerace C., Giallongo T., Di Giulio A.M., Gorio A. *Minimal manipulation of tissues and stem cells to achieve application in regenerative medicine.* Convegno monotematico SIF (Societa Italiana di Farmacologia). Titolo: "La farmacologia clinica tra impegno nella ricerca e ruolo nel Servizio Sanitario Nazionale". Napoli, 2-3 ottobre 2014

- Carelli S., Messaggio F., Giallongo T., **Caremoli F.**, Hebda D.M., Colli M., Tremolada C., Trabucchi E., Di Giulio A.M., Gorio A. *Fresh and Frozen Lipogems-derived micro-fractured human adipose tissue generates mesenchymal stem cells with higher differentiation potential and in vivo repair efficacy*. Congress of the Italian Society of Pharmacology (SIF), 2013, Torino.

- Carelli S., Messaggio F., Giallongo T., **Caremoli F.**, Hebda D.M., Colli M., Tremolada C., Trabucchi E., Di Giulio A.M., Gorio A. *Fresh and Frozen Lipogems-derived micro-fractured human adipose tissue generates mesenchymal stem cells with higher differentiation potential and* in vivo *repair efficacy.* International Society of Plastic Regenerative Surgery (ISPRES), 2013, Berlin.

- Bassoli A., Borgonovo G., Morini G., **Caremoli, F.**, Resta D., Arnoldi A., Boschin G. *Bioactive molecules from bulbs of* Muscari comosum *(Lampascioni)*; Italian Society of Nutraceutic (SINUT), 2012 Milan

Newspaper articles (Italian only):

- **Caremoli F.**, Bassoli A, Borgonovo G., Morini G., Torri L. *Il Gusto amaro: amarofili o amarofobi? Oltre all'intensità del gusto amaro, altri fattori specifici per ogni alimento potrebbero modularne la percezione.* Intersezioni. 2012.

  http://www.intersezioni.eu/public/art_321/24%20Alimentazione%20Caremoli%20et%20al..pdf

- **Caremoli F.** *Cellule portentose: Le cellule staminali avrebbero un ruolo determinante nella cura delle malattie neurodegenerative. Nuove prospettive per i ricercatori*. Intersezioni. 2013.

  http://www.intersezioni.eu/public/art_384/28%20Biotecnologie%20Caremoli.pdf

Ringraziamenti

I primi, doverosi, ringraziamenti vanno al Professor Gorio, per avermi dato questa enorme possibilità tre anni fa, scommettendo su di me e credendo nelle mie possibilità. Tutto il gruppo con cui ho lavorato, poi, mi ha accolto meravigliosamente e mi ha dato la possibilità di crescere come persona e come scienziato: in particolare voglio ringraziare Stephana per gli insegnamenti di questi tre anni, che porterò con me come bagaglio in qualunque situazione, lavorativa e non.

Tante cose sono cambiate in questi tre anni, ma il legame con la mia famiglia è diventato ancora più forte: grazie quindi a mia madre Marina, mio padre Edoardo, mia sorella Barbara e mio fratello Tommaso. Mi avete sempre supportato, sostenuto, aiutato, consigliato e, soprattutto, amato, anche nei momenti difficili che abbiamo passato e che stiamo passando (*per aspera sic itur ad astra*).

Graie aI miei compagni di avventura, i figli della ...serva: Toniella, che ha condiviso con me questo percorso di crescita, Anthea, dalla quale ho imparato più di quanto io le abbia insegnato (e non parlo solo di lavoro), e Claudio per tutti i momenti passati insieme, per l'impegno e l'energia che mi avete sempre dato!

Grazie alla collega Marianna, a Neva, Isabella e Alberto, e alle mie sorelle Giulia e Silvia, fenomenali compagni di viaggio e amici di una vita.

Grazie a Francesco, nuotatore provetto, amico e scienziato che si è fatto in quattro per aiutarmi e supportarmi.

Grazie a tutti gli amici e i colleghi del DISS: ringrazio soprattutto Alessandra, Elena, Silvia, Elisa, Valentina, Zuzana, Martina, Eleonora, Renata, Maria Teresa e Paola.

Grazie a Marco, infine, per esserci sempre, per starmi accanto e per darmi le emozioni più belle che si possano volere a questo mondo.

Condensare tre anni: tre lunghi anni di studio, lavoro, esperienze e amicizie, in poche righe non è sicuramente semplice. A tutti voi che mi siete stati vicini dico quindi: grazie!

Filippo